

Computer assisted proofs for transverse collision and near collision orbits in the restricted three body problem

Maciej J. Capiński¹

AGH University of Science and Technology, al. Mickiewicza 30, 30-059 Kraków, Poland

Shane Kepley

Vrije Universiteit Amsterdam, De Boelelaan 1105, 1081 HV Amsterdam, Netherlands

J.D. Mireles James²

Florida Atlantic University, 777 Glades Road, Boca Raton, Florida, 33431

Abstract

This paper considers two point boundary value problems for conservative systems defined in multiple coordinate systems, and develops a flexible a-posteriori framework for computer assisted existence proofs. Our framework is applied to the study collision and near collision orbits in the circular restricted three body problem. In this case the coordinate systems are the standard rotating coordinates, and the two Levi-Civita coordinate systems regularizing collisions with each of the massive primaries. The proposed framework is used to prove the existence of a number of orbits which have long been studied numerically in the celestial mechanics literature, but for which there are no existing analytical proofs at the mass and energy values considered here. These include transverse ejection/collisions from one primary body to the other, Strömberg's asymptotic periodic orbits (transverse homoclinics for $L_{4,5}$), families of periodic orbits passing through collision, and orbits connecting L_4 to ejection or collision.

Keywords: Celestial mechanics, collisions, transverse homoclinic, computer assisted proofs.

2010 MSC: 37C29, 37J46, 70F07.

1. Introduction

The present work develops computer assisted arguments for proving theorems about collision and near collision orbits in conservative systems, and applies these arguments

¹M. C. was partially supported by the NCN grants 2019/35/B/ST1/00655 and 2021/41/B/ST1/00407.

²J.D.M.J. was partially supported by NSF Grant DMS 1813501

Email addresses: `maciej.capinski@agh.edu.pl` (Maciej J. Capiński), `s.kepley@vu.nl` (Shane Kepley), `jmirelesjames@fau.edu` (J.D. Mireles James)

Preprint submitted to Elsevier

May 8, 2022

to a number of questions involving the planar circular restricted three body problem (PCRTBP). The PCRTBP, defined formally in Section 3, describes the motion of an infinitesimal particle like a satellite, asteroid, or comet moving in the field of two massive bodies called the primaries. These primary bodies are assumed to orbit their center of mass on Keplerian circles. Changing to a co-rotating frame of reference results in autonomous equations of motion, and choosing normalized units of distance, mass, and time reduces the number of parameters in the problem to one: the mass ratio of the primaries.

We consider the following questions about the dynamics of the infinitesimal body in the PCRTBP. In each case we are interested in non-perturbative values of the mass and energy parameters. Recall that in systems which conserve energy, periodic orbits occur in one parameter families – or tubes – parameterized by energy. We note also that the PCRTBP has an equilibrium solution, or Lagrange point, called L_4 in the upper half plane forming an equilateral triangle with the two primaries. (Similarly, L_5 forms an equilateral triangle in the lower half plane).

We develop a methodology which allows us to address the following questions.

- **Q1:** *Do there exist orbits of the infinitesimal body, which collide with one primary in forward time, and the other primary in backward time?* We refer to such orbits as primary-to-primary ejection-collisions.
- **Q2:** *Do there exist orbits of infinitesimal body which are asymptotic to the L_4 in backward time, but which collide with a primary in forward time?* (Or the reverse - from ejection to L_4). We refer to these as L_4 -to-collision orbits (or ejection-to- L_4 orbits).
- **Q3:** *Do there exist orbits of the infinitesimal body which are asymptotic in both forward and backward time to L_4 ?* Such orbits are said to be homoclinic to L_4 .
- **Q4:** *Do there exist tubes of large amplitude periodic orbits for the infinitesimal body, which accumulate to an ejection-collision orbit with one of the primaries?* Such tubes are said to terminate at an ejection-collision orbit.
- **Q5:** *Do there exist tubes of periodic orbits for the infinitesimal body which accumulate to a pair of ejection-collision orbits going from one primary to the other and back?.* Such tubes are said to terminate at a consecutive ejection-collision.

In response to the questions above we have the following theorems, which constitute the main results of the present work.

Theorem 1. *For the PCRTBP with mass ratio 1/3 there exist ejection-collision orbits from one primary to the other, in both directions. (See page 31 for the precise statement.)*

Theorem 2. *For the PCRTBP with equal masses, there exist ejection-to- L_4 orbits, and L_4 -to-collision orbits. (See page 34 for the precise statement.) Analogous orbits exist for L_5 by symmetry considerations.*

Theorem 3. *For the PCRTBP with equal masses, there exist transverse homoclinic orbits for L_4 . (See page 36 for the precise statement.) Analogous orbits exist for L_5 by symmetry considerations.*

Theorem 4. *For the PCRTBP with Earth-Moon mass parameter, there exists a family of periodic orbits which accumulate to an ejection-collision orbit involving the Earth. The ejection-collision orbit has “large amplitude” in the sense that it passes near collision with the Moon. (See page 38 for the precise statement.)*

Theorem 5. *For the PCRTBP with equal masses, there exists a family of periodic orbits which accumulate to a consecutive ejection-collision orbit involving both primaries. (See page 39 for the precise statement.)*

Remark 6 (Termination orbits). Theorems 3,4,5 involve the termination of tubes of periodic orbits. In the case of Theorem 3, the existence of a transverse L_4 homoclinic implies the further existence of a family of periodic orbits which accumulates to the L_4 homoclinic by a theorem of Henrard [1]. It is worth remarking further that the orbits of Theorem 3 imply also the existence of chaotic dynamics in the L_4 energy level. This is due to a theorem of Devaney [2]. In Theorems 4 and 5, we obtain families of periodic orbits terminating at the ejection-collision orbit by a direct application of the implicit function theorem.

Termination orbits have a long history in celestial mechanics, and are of fundamental importance in equivariant bifurcation theory. We refer the interested reader to the discussion of “Strömberg’s termination principle” in Chapter 9 of [3], and to the works of [4, 5, 6] on equivariant families in the Hill three body and restricted three body problems. See also the works of [7, 8] on global continuation families in the restricted N -body problem.

Remark 7 (Ballistic transport). Theorem 1 establishes the existence of ballistic transport, or a zero energy transfer, from one primary to the other in finite time. The existence of ballistic transport shows for example that debris can diffuse between a planet and its moon, or between a star and one of its planets, using only the natural dynamics of the system. This phenomena is observed for example when Earth rocks, ejected into space after a meteor strike, are later found on the Moon [9] (or vice versa). In a similar fashion, Theorem 2 shows the existence of orbits whose velocity limits to zero in backward time, but to infinity in finite forward time (or vice versa). Such orbits describe ballistic transfer from L_4 to a primary.

Remark 8 (Moulton’s L_4 periodic orbits). The family of periodic orbits whose existence is established in Theorem 5 are of Moulton’s L_4 type, in the sense of [10]. That is, these are periodic orbits which when projected into the (x, y) plane (i.e. the configuration space) have non-trivial winding about L_4 . See also Chapter 9 of [3], or the works of [11, 12] for a more complete discussion of the history (and controversy) surrounding Moulton’s orbits. The present work provides the first mathematically rigorous proof that Moulton type L_4 periodic orbits exist.

Each of the five theorems above are proven using a common analytical set up for two point boundary value problems (BVPs) in energy manifolds of systems defined in several different coordinate systems. Our setup for the BVPs is designed to allow for rigorous computer assisted validation of the needed assumptions using interval arithmetic. This is implemented using freely available validated numerical tools for computing mathematically rigorous enclosures of solutions of initial value problems, variational equations, and

invariant manifolds. In particular, we make extensive use of the CAPD library for validated numerical integration of ODEs [13]. (Additional details about these algorithms are found in [14, 15]. Similar methods for computing validated enclosures of stable/unstable manifolds attached to equilibrium solutions are discussed in [16, 17].)

Collisions and near collision orbits are incorporated into this analytical setup via the classical Levi-Civita regularization. In these coordinates the set of all collisions appears as a simple one dimensional manifold, which we refer to as the collision set [18]. Once we obtain the collision set analytically we formulate BVPs for orbits beginning and ending at collision. We review the Levi-Civita coordinates for the PCRTBP in Section 3, and refer the interested reader to Chapter 3 of [3], to the notes of [19, 20], and to the works of [21, 22, 23] for much more complete overview of regularization in celestial mechanics.

Remark 9 (Collisions in the literature). Collisions are an essential and delicate topic in celestial mechanics. While it has been shown that the set of orbits which collide in finite time has measure zero [24, 25], it is also known that the embedding of the collision set may be topologically complicated. For example, recent results of [26] show that there exist open sets where collisions are dense. Many mathematically rigorous theorems on the existence of collisions exploit perturbative techniques, taking one or more of the masses to be small [27, 28, 29, 30, 31], or the energy to be large [32, 33, 34, 35, 35, 36, 37, 38, 39, 40]. These works depend on results from geometry/topology, the calculus of variations, and the KAM theory. For parameter and energy regimes where analytical results are unavailable, numerical studies illuminate the dynamics of the collision set [41, 42, 43, 44, 45, 46, 47, 48]. Our work goes towards providing a framework for computer assisted proofs for collision orbits, for the parameter regimes where the perturbative methods cannot be applied.

Remark 10 (CAPs in the literature). Constructive computer assisted arguments have been used to prove many theorems in celestial mechanics. An overview of the literature on computer assisted proofs (CAPs) in celestial mechanics is beyond the scope of the present paper, and we refer the interested reader to the works of [49, 50, 51, 52, 53] on periodic orbits, the works of [54, 55, 56, 16, 57] on connecting orbits and chaos, the works of [58, 59, 60, 61] on oscillations to infinity, center manifolds, and Arnold diffusion, and the works of [62, 63, 64, 65, 66] on quasi-periodic orbits and KAM phenomena. By looking also to the references in the papers cited in this paragraph, the interested reader will come away with a deeper appreciation of the role of CAPs in celestial mechanics. We remark that, until now, collisions have been viewed largely as impediments to the implementation of CAPs. We demonstrate in the current paper that this is not the case.

The remainder of the paper is organized as follows. In Section 2 we describe the problem setup in terms of an appropriate multiple shooting problem, and establish tools for solving the problem. In particular, we define the unfolding parameters which we use to isolate transverse solutions in energy level sets and use this notion to formulate Theorem 15 and Lemma 18 which we later use for our computer assisted proofs. In Section 3 we describe the PCRTBP and its Levi-Civita regularization. Sections 4, 5, and 6 describe respectively the formulation of the multiple shooting problem for primary-to-primary ejection-collision orbits, L_4 to ejection/collision orbits, L_4 homoclinic orbits, and periodic ejection-collision families. Section 7 describes our computer assisted proof

strategy and illustrates how this strategy is used to prove our main theorems. Some technical details are given in the appendices. The codes implementing the computer assisted proofs discussed in this paper are available at the homepage of the first author MC.

2. Problem setup

Consider an ODE with one or more first integrals or constants of motion. For such systems, the level sets of the integrals give rise to invariant sets. Indeed, the level sets are invariant manifolds except at critical points of the conserved quantities. In this section we describe a shooting method for two point boundary value problems between submanifolds of the level set. To be more precise, we consider two manifolds, parameterized (locally) by some functions, which are contained in a level set. We present a method which allows us to find points on these manifold which are linked by a solution of an ODE. This in particular implies that the two manifolds intersect. Our method will allow us to establish transversality of the intersection within the level set.

We consider an ODE

$$x' = f(x), \quad (1)$$

where $f : \mathbb{R}^d \rightarrow \mathbb{R}^d$. Assume that the flow $\phi(x, t)$ induced by (1) has an integral of motion expressed as

$$E : \mathbb{R}^d \rightarrow \mathbb{R}^k,$$

which means that

$$E(\phi(x, t)) = E(x), \quad (2)$$

for every $x \in \mathbb{R}^d$ and $t \in \mathbb{R}$. Fix $c \in \mathbb{R}^k$ and define the level set

$$M := \{x \in \mathbb{R}^d : E(x) = c\}, \quad (3)$$

and assume that M is (except possibly at some degenerate points) a smooth manifold. Consider two open sets $D_1 \subset \mathbb{R}^{d_1}$ and $D_2 \subset \mathbb{R}^{d_2}$ and two chart maps

$$P_i : D_i \rightarrow M \subset \mathbb{R}^d \quad \text{for } i = 1, 2, \quad (4)$$

parameterizing submanifolds of M .

Remark 11. *One can for example think of the P_1 and P_2 as parameterizations of the exit or entrance sets on some local unstable and stable manifolds, respectively, of some invariant object. However in some of the applications to follow $P_{1,2}$ will parameterize collision sets in regularized coordinates or some surfaces of symmetry for f .*

We seek points $\bar{x}_i \in D_i$ for $i = 1, 2$ and a time $\bar{\tau} \in \mathbb{R}$ such that

$$\phi(P_1(\bar{x}_1), \bar{\tau}) = P_2(\bar{x}_2). \quad (5)$$

Note that if P_1 and P_2 parameterize some ϕ -invariant manifolds, then Equation (5) implies that these manifolds intersect. The setup is depicted in Figure 1.

Remark 12. *Denote by x_1, x_2 the points $x_1 \in \mathbb{R}^{d_1}$ and by $x_2 \in \mathbb{R}^{d_2}$: this avoids confusion with $x \in \mathbb{R}^d$.*

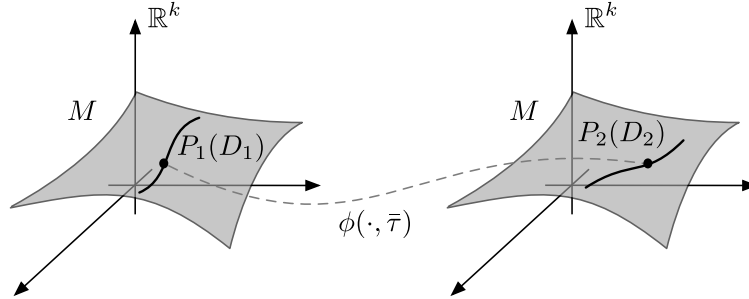


Figure 1: The left and right plots are in \mathbb{R}^d with a $d - k$ dimensional manifold M depicted in gray. The manifolds $P_i(D_i) \subset M$, for $i = 1, 2$, are represented by curves inside of M . We seek $\bar{x}_1 \in D_1, \bar{x}_2 \in D_2$ and $\bar{\tau} \in \mathbb{R}$ such that $\phi(P_1(\bar{x}_1), \bar{\tau}) = P_2(\bar{x}_2)$. The two points $P_i(\bar{x}_i)$, for $i = 1, 2$, are represented by dots.

We introduce a general scheme which allows us to:

1. Establish the intersection of the manifolds parameterized by P_1 and P_2 by means of a suitable Newton operator.
2. Establish that the intersection is transverse relative to the level set M .
3. Provide a setup flexible enough for multiple shooting between charts in different coordinates.

Our methodology is applied to establish connections between stable/unstable and collision manifolds in the PCRTBP.

2.1. Level set shooting

We now provide a more detailed formulation of problem (5) which allows us to describe connections between multiple level sets in distinct coordinate systems (instead of just one coordinate system as discussed in Section 3). This allows us to study applications to collision dynamics as boundary value problems joining points in different coordinate systems. Let $U_1, U_2 \subset \mathbb{R}^d$ be open sets and consider smooth functions E_1, E_2

$$E_i : U_i \rightarrow \mathbb{R}^k \quad \text{for } i = 1, 2,$$

for which $DE_i(x)$ is of rank k for every $x \in U_i$, for $i = 1, 2$. We fix $c_1, c_2 \in \mathbb{R}^k$ and define the following level sets

$$M_i = \{x \in U_i : E_i(x) = c_i\} \quad \text{for } i = 1, 2,$$

and assume that $M_i \neq \emptyset$ for $i = 1, 2$. Observe that the M_i are smooth $d - k$ dimensional manifolds by the assumption that DE_i are of rank k , for $i = 1, 2$.

Consider now a smooth function $R : U_1 \times \mathbb{R} \times \mathbb{R}^k \rightarrow \mathbb{R}^d$. We introduce the following notation for coordinates

$$(x, \tau, \alpha) \in \mathbb{R}^d \times \mathbb{R} \times \mathbb{R}^k, \quad y \in \mathbb{R}^d,$$

and define a parameter dependent family of maps $R_{\tau, \alpha} : U_1 \rightarrow \mathbb{R}^d$ by

$$R_{\tau, \alpha}(x) := R(x, \tau, \alpha),$$

and assume that for each $(x, \tau, \alpha) \in \mathbb{R}^{d+k+1}$, the $d \times d$ matrix

$$\frac{\partial}{\partial x} R(x, \tau, \alpha),$$

is invertible, so that $R_{\tau, \alpha}(x)$ is a local diffeomorphism on \mathbb{R}^d .

The following definition makes precise our assumptions about when $R_{\tau, \alpha}(x)$ takes values in M_2 .

Definition 13. *We say that α is an unfolding parameter for R if the following two conditions are satisfied for every $x \in M_1$.*

1. *If $R_{\tau, \alpha}(x) \in M_2$, then $\alpha = 0$.*
2. *If $R_{\tau, 0}(x) \in U_2$, then $R_{\tau, 0}(x) \in M_2$.*

To emphasize that we are interested in points mapped from M_1 to M_2 , we say that α is an unfolding parameter for R from M_1 to M_2 .

Assume from now on that α is an unfolding parameter for R . We consider two open sets $D_1 \subset \mathbb{R}^{d_1}$ and $D_2 \subset \mathbb{R}^{d_2}$ where $d_1, d_2 \in \mathbb{N}$ and two smooth functions

$$P_i : D_i \rightarrow M_i, \quad \text{for } i = 1, 2,$$

each of which is a diffeomorphism onto its image. Define

$$F : D_1 \times D_2 \times \mathbb{R} \times \mathbb{R}^k \rightarrow \mathbb{R}^d$$

by the formula

$$F(x_1, x_2, \tau, \alpha) := R_{\tau, \alpha}(P_1(x_1)) - P_2(x_2). \quad (6)$$

We require that

$$d_1 + d_2 + 1 + k = d, \quad (7)$$

and seek $\bar{x}_1, \bar{x}_2, \bar{\tau}$ such that

$$F(\bar{x}_1, \bar{x}_2, \bar{\tau}, 0) = R_{\bar{\tau}, 0}(P_1(\bar{x}_1)) - P_2(\bar{x}_2) = 0, \quad (8)$$

with $DF(\bar{x}_1, \bar{x}_2, \bar{\tau}, 0)$ an isomorphism. In fact, we do more than simply solve (8). For some open interval $I \subset \mathbb{R}$ containing $\bar{\tau}$ we establish a transverse intersection between the smooth manifolds $R(P_1(D_1), I, 0)$ and $P_2(D_2)$ at $\bar{y} := P_2(\bar{x}_2) \in M_2$.

The setup above, and in particular the roles of the parameters α and τ , might appear puzzling. We now give an example which informs the intuition. In the applications we have in mind, τ is the time associated with the flow map of an ODE. The unfolding parameter α deals with the fact that we solve a problem restricted to the level sets M_i for $i = 1, 2$ though there are other practical methods to enforce this constraint.⁵ Consider the following example.

⁵Alternatives are to either fix the energy and use its formula to eliminate one of the variables in the equations of motion, or to work with coordinates in which we can write M_i as graphs of some functions and use these functions and appropriate projections to enforce the constraints. We believe that the approach with the unfolding parameter has the advantage that it simplifies formulas and easier to implement.

Example 14. (*Canonical unfolding.*) Consider the ODE in Equation (1) and $E : \mathbb{R}^d \rightarrow \mathbb{R}$ satisfying Equation (2). Suppose $c \in \mathbb{R}$ is fixed and denote its associated level set by $M := \{E = c\}$ (In this example we have $k = 1$ and $E_1 = E_2 = E$.) Assume there are smooth functions P_1, P_2 as in (4) and that $d_1 + d_2 + 2 = d$. We construct a shooting operator for Equation (5) by choosing R as follows. Consider the α -parameterized family of ODEs

$$x' = f(x) + \alpha \nabla E(x).$$

Let $\phi_\alpha(x, t)$ denote the induced flow and note that $\phi_0 = \phi$ is the flow induced by Equation (1). Defining the shooting operator by the formula

$$R(x, \tau, \alpha) := \phi_\alpha(x, \tau), \quad (9)$$

we see that solving Equation (5) is equivalent to solving Equation (8).

Observe that α is unfolding for R because E is an integral of motion for ϕ from which it follows that

$$\begin{aligned} \frac{d}{dt} E(R_{\tau, \alpha}(x)) &= \frac{d}{dt} E(\phi_\alpha(x, t)) \\ &= \nabla E(\phi_\alpha(x, t)) \cdot (f(\phi_\alpha(x, t)) + \alpha \nabla E(\phi_\alpha(x, t))) \\ &= \alpha \|\nabla E(\phi_\alpha(x, t))\|^2, \end{aligned}$$

where \cdot denotes the standard scalar product. Here we have used the fact that Equation (2) implies $\nabla E(x) \cdot f(x) = 0$ but also $\nabla E(\phi_\alpha(x, t)) \neq 0$ since ∇E is assumed to have rank 1 everywhere.

Returning to the general setup we have the following theorem.

Theorem 15. Assume that α is an unfolding parameter for R and F is defined as in Equation (6). If

$$F(\bar{x}_1, \bar{x}_2, \bar{\tau}, \bar{\alpha}) = 0, \quad (10)$$

then $\bar{\alpha} = 0$. Moreover, if $DF(\bar{x}_1, \bar{x}_2, \bar{\tau}, 0)$ is an isomorphism, then there exists an open interval $I \subset \mathbb{R}$ of $\bar{\tau}$ such that the manifolds $R(P_1(D_1), I, 0)$ and $P_2(D_2)$ intersect transversally in M_2 at $\bar{y} := P_2(\bar{x}_2)$. Specifically, we have the splitting

$$T_{\bar{y}}R(P_1(D_1), I, 0) \oplus T_{\bar{y}}P_2(D_2) = T_{\bar{y}}M_2, \quad (11)$$

and moreover, \bar{y} is an isolated transverse point.

Proof. Recalling the definition of F in Equation (6) and the hypothesis of Equation (10), we have that $\bar{x} = P_1(\bar{x}_1) \in M_1$ and $\bar{y} = P_2(\bar{x}_2) \in M_2$. The fact that α is an unfolding parameter for R , combined with $R(\bar{x}, \bar{\tau}, \bar{\alpha}) = \bar{y}$, implies that $\bar{\alpha} = 0$. Since $F(\bar{x}_1, \bar{x}_2, \bar{\tau}, 0) = 0$, we see that $R(P_1(D_1), I, 0)$ and $P_2(D_2)$ intersect at \bar{y} .

Our hypotheses on $P_{1,2}$ and R imply that $R(P_1(D_1), I, 0)$ and $P_2(D_2)$ are submanifolds of M_2 so evidently

$$T_{\bar{y}}R(P_1(D_1), I, 0) \oplus T_{\bar{y}}P_2(D_2) \subset T_{\bar{y}}M_2.$$

However, from the assumption in Equation (7) we have $d - k = d_1 + d_2 + 1$ and therefore it suffices to prove that $T_{\bar{y}}R(P_1(D_1), I, 0) \oplus T_{\bar{y}}P_2(D_2)$ is $d - k$ dimensional.

Suppose $\{e_1, \dots, e_{d_1}\}$ is a basis for \mathbb{R}^{d_1} and $\{\tilde{e}_1, \dots, \tilde{e}_{d_2}\}$ is a basis for \mathbb{R}^{d_2} . Define

$$\begin{aligned} v_i &:= \frac{\partial R}{\partial x_1}(\bar{x}_1, \bar{\tau}, 0) DP_1(\bar{x}_1) e_i & \text{for } i = 1, \dots, d_1 \\ v_i &:= DP_2(\bar{x}_2) \tilde{e}_{i-d_1} & \text{for } i = d_1 + 1, \dots, d_1 + d_2 \\ v_{d_1+d_2+1} &:= \frac{\partial R}{\partial \tau}(\bar{x}_1, \bar{\tau}, 0). \end{aligned}$$

After differentiating Equation (6) we obtain the formula

$$DF = \begin{pmatrix} \frac{\partial F}{\partial x_1} & \frac{\partial F}{\partial x_2} & \frac{\partial F}{\partial \tau} & \frac{\partial F}{\partial \alpha} \end{pmatrix} = \begin{pmatrix} \frac{\partial R}{\partial x_1} DP_1 & -DP_2 & \frac{\partial R}{\partial \tau} & \frac{\partial R}{\partial \alpha} \end{pmatrix},$$

and since DF is an isomorphism at $(\bar{x}_1, \bar{x}_2, \bar{\tau}, 0)$, it follows that the vectors $v_1, \dots, v_{d_1+d_2+1}$ span a $d_1 + d_2 + 1 = d - k$ dimensional space. Observe that

$$\begin{aligned} T_{\bar{y}}R(P(D_1), I, 0) &= \text{span}(v_1, \dots, v_{d_1}, v_{d_1+d_2+1}), \\ T_{\bar{y}}P_2(D_2) &= \text{span}(v_{d_1+1}, \dots, v_{d_1+d_2}), \end{aligned}$$

proving the claim in Equation (11). Moreover, since

$$\dim R(P_1(D_1), I, 0) + \dim P_2(D_2) = (d_1 + 1) + d_2 = d - k = \dim M_2,$$

it follows that \bar{y} is an isolated transverse intersection point which concludes the proof. \blacksquare

We finish this section by defining an especially simple ‘‘dissipative’’ unfolding parameter which works in the setting of the PCRTBP.

Example 16. (*Dissipative unfolding.*) Let $x, y \in \mathbb{R}^{2k}$, let $\Omega : \mathbb{R}^{2k} \rightarrow \mathbb{R}$ and $J \in \mathbb{R}^{2k \times 2k}$ be of the form

$$J = \begin{pmatrix} 0 & \text{Id}_k \\ -\text{Id}_k & 0 \end{pmatrix},$$

where Id_k is a $k \times k$ identity matrix. Let us consider an ODE of the form

$$(x', y') = f(x, y) := \left(y, 2Jy + \frac{\partial}{\partial x} \Omega(x) \right).$$

One can check that $E(x, y) = -\|y\|^2 + 2\Omega(x)$ is an integral of motion. Consider the parameterized family of ODEs

$$(x', y') = f_\alpha(x, y) := f(x, y) + (0, \alpha y), \quad (12)$$

and let $\phi_\alpha((x, y), t)$ denote the flow induced by Equation (12). Define the shooting operator defined by

$$R((x, y), \tau, \alpha) := \phi_\alpha((x, y), \tau). \quad (13)$$

As in Example 14, one can check the equivalence between Equations (5) and (8). The fact that α is unfolding for R follows as

$$\frac{d}{dt} E(\phi_\alpha((x, y), t)) = -2\alpha \|y\|^2.$$

2.2. Level set multiple shooting

Consider a sequence of open sets $U_1, \dots, U_n \subset \mathbb{R}^d$ and a sequence of smooth maps

$$E_i : U_i \rightarrow \mathbb{R}^k \quad \text{for } i = 1, \dots, n$$

for which $DE_i(x)$ is of rank k for every $x \in U_i$, for $i = 1, \dots, n$. Let $c_1, \dots, c_n \in \mathbb{R}^k$ be a fixed sequence with corresponding level sets

$$M_i := \{x \in U_i : E_i(x) = c_i\} \quad \text{for } i = 1, \dots, n.$$

Let

$$R^i : U_i \times \mathbb{R} \times \mathbb{R}^k \rightarrow \mathbb{R}^d \quad \text{for } i = 1, \dots, n-1$$

be a sequence of smooth functions which defines a sequence of parameter dependent maps

$$\begin{aligned} R_{\tau, \alpha}^i &: U_i \rightarrow \mathbb{R}^d, \\ R_{\tau, \alpha}^i(x) &:= R^i(x, \tau, \alpha), \quad \text{for } i = 1, \dots, n-1. \end{aligned}$$

We assume that for each fixed τ and α , each of the maps is a local diffeomorphism on \mathbb{R}^d .

Let $D_0 \subset \mathbb{R}^{d_0}$ and $D_n \subset \mathbb{R}^{d_n}$ be open sets, and let

$$P_0 : D_0 \rightarrow M_0 \subset \mathbb{R}^d, \quad P_n : D_n \rightarrow M_n \subset \mathbb{R}^d,$$

be diffeomorphisms onto their image. Assume that

$$d_0 + d_n + 1 + k = d \tag{14}$$

and consider the function

$$\tilde{F} : \mathbb{R}^{nd} \supset D_0 \times \underbrace{\mathbb{R}^d \times \dots \times \mathbb{R}^d}_{n-1} \times D_n \times \mathbb{R} \times \mathbb{R}^k \rightarrow \underbrace{\mathbb{R}^d \times \dots \times \mathbb{R}^d}_n,$$

defined by the formula

$$\tilde{F}(x_0, \dots, x_n, \tau, \alpha) = \begin{pmatrix} P_0(x_0) - x_1 \\ R_{\tau, \alpha}^1(x_1) - x_2 \\ \vdots \\ R_{\tau, \alpha}^{n-2}(x_{n-2}) - x_{n-1} \\ R_{\tau, \alpha}^{n-1}(x_{n-1}) - P_n(x_n) \end{pmatrix} \tag{15}$$

We now define the following functions

$$\begin{aligned} R &: U_1 \times \mathbb{R} \times \mathbb{R}^k \rightarrow \mathbb{R}^d, \\ F &: D_0 \times D_n \times \mathbb{R} \times \mathbb{R}^k \rightarrow \mathbb{R}^d \end{aligned}$$

by the formulas

$$\begin{aligned} R(x_1, \tau, \alpha) &= R_{\tau, \alpha}(x_1) := R_{\tau, \alpha}^{n-1} \circ \dots \circ R_{\tau, \alpha}^1(x_1), \\ F(x_0, x_n, \tau, \alpha) &:= R_{\tau, \alpha}(P_0(x_0)) - P_n(x_n). \end{aligned} \tag{16}$$

Definition 17. We say that α is an unfolding parameter for the sequence $R_{\tau,\alpha}^i$ if it is unfolding for $R_{\tau,\alpha} = R_{\tau,\alpha}^{n-1} \circ \dots \circ R_{\tau,\alpha}^1$.

We now formulate the following lemma.

Lemma 18. If $\tilde{F}(\bar{x}_0, \dots, \bar{x}_n, \bar{\tau}, \bar{\alpha}) = 0$ and $D\tilde{F}(\bar{x}_0, \dots, \bar{x}_n, \bar{\tau}, \bar{\alpha})$ is an isomorphism, then $F(\bar{x}_0, \bar{x}_n, \bar{\tau}, \bar{\alpha}) = 0$ and $DF(\bar{x}_0, \bar{x}_n, \bar{\tau}, \bar{\alpha})$ is an isomorphism.

Proof. The fact that $F(\bar{x}_0, \bar{x}_n, \bar{\tau}, \bar{\alpha}) = 0$ follows directly from the way \tilde{F} and F are defined in Equations (15) and (16) respectively. Before proving that DF is an isomorphism, we set up some notation. We will write

$$dR^i := \frac{\partial R^i}{\partial x_i}(\bar{x}_i, \bar{\tau}, \bar{\alpha}) \quad \text{for } i = 1, \dots, n-1.$$

It will be convenient for us to swap the order of the coordinates, so we define

$$\hat{F}(x_1, \dots, x_n, x_0, \tau, \alpha) := \tilde{F}(x_0, x_1, \dots, x_n, \tau, \alpha), \quad (17)$$

and write

$$\hat{F} = \left(\hat{F}_1, \dots, \hat{F}_n \right) \quad \text{where} \quad \hat{F}_i : \mathbb{R}^{nd} \rightarrow \mathbb{R}^d, \text{ for } i = 1, \dots, n.$$

Finally, the last notation we introduce is $z \in \mathbb{R}^d$ to combine the coordinates from the domain of F together

$$z = (z_1, \dots, z_d) = (x_n, x_0, \tau, \alpha) \in \mathbb{R}^{d_n} \times \mathbb{R}^{d_0} \times \mathbb{R} \times \mathbb{R}^k = \mathbb{R}^d.$$

Note that z is also the variable corresponding to the last d coordinates from the domain of \hat{F} (see Equation (17)). Finally, we remark that all derivatives considered in the argument below are computed at the point $(\bar{x}_0, \dots, \bar{x}_n, \bar{\tau}, \bar{\alpha})$.

With the above notation we see that

$$D\hat{F} = \begin{pmatrix} -\text{Id} & 0 & \dots & 0 & \frac{\partial \hat{F}_1}{\partial z} \\ dR^1 & -\text{Id} & \ddots & \vdots & \frac{\partial \hat{F}_2}{\partial z} \\ 0 & \ddots & \ddots & 0 & \vdots \\ \vdots & \ddots & dR^{n-2} & -\text{Id} & \frac{\partial \hat{F}_{n-1}}{\partial z} \\ 0 & \dots & 0 & dR^{n-1} & \frac{\partial \hat{F}_n}{\partial z} \end{pmatrix},$$

and $D\hat{F}$ is an isomorphism since $D\tilde{F}$ is an isomorphism. To see this define a sequence of vectors $v^1, \dots, v^d \in \mathbb{R}^{nd}$ of the form

$$v^i = \begin{pmatrix} v_1^i \\ \vdots \\ v_n^i \end{pmatrix} \in \mathbb{R}^d \times \dots \times \mathbb{R}^d = \mathbb{R}^{nd} \quad \text{for } i = 1, \dots, d,$$

with $v_1^i, v_n^i \in \mathbb{R}^d$ chosen as

$$v_1^i = \frac{\partial \hat{F}_1}{\partial z_i}, \quad v_n^i = \begin{pmatrix} 0 & \dots & 0 & \overset{i}{1} & 0 & \dots & 0 \end{pmatrix}^\top, \quad (18)$$

and $v_2^i, \dots, v_{n-1}^i \in \mathbb{R}^d$ defined inductively as

$$v_k^i = dR^{k-1}v_{k-1}^i + \frac{\partial \hat{F}_k}{\partial z_i} \quad \text{for } k = 2, \dots, n-1. \quad (19)$$

Note that from the choice of v_n^i in (18) the vectors v^1, \dots, v^d are linearly independent.

By direct computation⁶ it follows that

$$D\hat{F}v^i = \begin{pmatrix} 0 \\ dR^{n-1}v_{n-1}^i + \frac{\partial \hat{F}_n}{\partial z_i} \end{pmatrix} \quad \text{for } i = 1, \dots, d, \quad (20)$$

where the zero is in $\mathbb{R}^{(n-1)d}$.

Looking at (15), since $\hat{F}_1, \dots, \hat{F}_{n-1}$ do not depend on x_n , we see that for $i \in \{1, \dots, d_n\}$ we have $\frac{\partial \hat{F}_1}{\partial z_i} = \dots = \frac{\partial \hat{F}_{n-1}}{\partial z_i} = 0$, so

$$\begin{aligned} dR^{n-1}v_{n-1}^i + \frac{\partial \hat{F}_n}{\partial z_i} &= dR^{n-1} \left(dR^{n-2}v_{n-2}^i + \frac{\partial \hat{F}_{n-1}}{\partial z_i} \right) - \frac{\partial P_n}{\partial x_{n,i}} \\ &= dR^{n-1} (dR^{n-2}v_{n-2}^i + 0) - \frac{\partial P_n}{\partial x_{n,i}} \\ &= \dots \\ &= dR^{n-1} \dots dR^1 v_1^i - \frac{\partial P_n}{\partial x_{n,i}} \\ &= dR^{n-1} \dots dR^1 \frac{\partial \hat{F}_1}{\partial z_i} - \frac{\partial P_n}{\partial x_{n,i}} \\ &= -\frac{\partial P_n}{\partial x_{n,i}} \quad \text{for } i = 1, \dots, d_n. \end{aligned} \quad (21)$$

Similarly, for $j = i - d_n \in \{1, \dots, d_0\}$ from (15) we see that $\frac{\partial \hat{F}_1}{\partial z_i} = \frac{\partial P_0}{\partial x_{0,j}}$ and $\frac{\partial \hat{F}_2}{\partial z_i} = \dots = \frac{\partial \hat{F}_n}{\partial z_i} = 0$, so

$$dR^{n-1}v_{n-1}^i + \frac{\partial \hat{F}_n}{\partial z_i} = dR^{n-1}dR^{n-2} \dots dR^1 \frac{\partial P_0}{\partial x_{0,j}} = \frac{\partial (R_{\tau, \bar{\alpha}} \circ P_0)}{\partial x_{0,j}} \quad (22)$$

for $i = d_n + 1, \dots, d_n + d_0$.

The index $i = d_n + d_0 + 1$ corresponds to τ . Similarly to (21), by inductively applying the chain rule, it follows that

$$dR^{n-1}v_{n-1}^i + \frac{\partial \hat{F}_n}{\partial z_i} = \frac{\partial R}{\partial \tau} \quad \text{for } i = d_n + d_0 + 1. \quad (23)$$

Finally, for $j = i - d_n - d_0 - 1 \in \{1, \dots, k\}$, the variable z_i corresponds to α_j , and also by applying the chain rule we obtain that

$$dR^{n-1}v_{n-1}^i + \frac{\partial \hat{F}_n}{\partial z_i} = \frac{\partial R}{\partial \alpha_j} \quad \text{for } i = d_n + d_0 + 2, \dots, d. \quad (24)$$

⁶From (15) and (19) follow the cancellations when multiplying the vector v^i by $D\hat{F}$.

Combining Equations (20)–(24) we see that

$$\left(D\hat{F}v^1 \quad \dots \quad D\hat{F}v^d \right) = \begin{pmatrix} 0 & 0 & 0 & 0 \\ -\frac{\partial P_n}{\partial x_n} & \frac{\partial(R_{\tau,\alpha} \circ P_0)}{\partial x_0} & \frac{\partial R}{\partial \tau} & \frac{\partial R}{\partial \alpha} \end{pmatrix}. \quad (25)$$

Since v^1, \dots, v^d are linearly independent and since $D\hat{F}$ is an isomorphism, the rank of the above matrix is d . Looking at Equation (15) we see that the lower part of the matrix in Equation (25) corresponds to DF which implies that DF is of rank d , hence is an isomorphism. ■

We see that we can validate assumptions of Theorem 15 by setting up a multiple shooting problem (15) and applying Lemma 18. To do so, one needs to additionally check whether α is an unfolding parameter for the sequence $R_{\tau,\alpha}^i$.

3. Regularization of collisions in the PCRTBP

In this section we formally introduce the equations of motion for the PCRTBP as discussed in Section 1. Recall that the problem describes a three body system, where two massive primaries are on circular orbits about their center of mass, and a third massless particle moves in their field. The equations of motion for the massless particle are expressed in a co-rotating frame with the frequency of the primaries. Writing Newton's laws in the co-rotating frame leads to

$$\begin{aligned} x'' &= 2y' + \partial_x \Omega(x, y), \\ y'' &= -2x' + \partial_y \Omega(x, y), \end{aligned} \quad (26)$$

where

$$\begin{aligned} \Omega(x, y) &= (1 - \mu) \left(\frac{r_1^2}{2} + \frac{1}{r_1} \right) + \mu \left(\frac{r_2^2}{2} + \frac{1}{r_2} \right), \\ r_1^2 &= (x - \mu)^2 + y^2, \quad \text{and} \quad r_2^2 = (x + 1 - \mu)^2 + y^2. \end{aligned}$$

Here x, y are the positions of the massless particle on the plane. The μ and $1 - \mu$ are the masses of the primaries (normalized so that the total mass of the system is 1). The rotating frame is oriented so that the primaries lie on the x -axis, with the center of mass at the origin. We take $\mu \in (0, \frac{1}{2}]$ so that the large body is always to the right of the origin. The larger primary has mass $m_1 = 1 - \mu$ and is located at the position $(\mu, 0)$. Similarly the smaller primary has mass $m_2 = \mu$ and is located at position $(\mu - 1, 0)$. The top frame of Figure 2 provides a schematic for the positioning of the primaries and the massless particle.

Let $U \subset \mathbb{R}^4$ denote the open set

$$U := \{(x, p, y, q) \in \mathbb{R}^4 \mid (x, y) \notin \{(\mu, 0), (\mu - 1, 0)\}\}.$$

The vector field $f: U \rightarrow \mathbb{R}^4$ defined by

$$f(x, p, y, q) := \begin{pmatrix} 2q + x - \frac{(1-\mu)(x-\mu)}{((x-\mu)^2+y^2)^{3/2}} - \frac{\mu(x+1-\mu)}{((x+1-\mu)^2+y^2)^{3/2}} \\ q \\ -2p + y - \frac{(1-\mu)y}{((x-\mu)^2+y^2)^{3/2}} - \frac{\mu y}{((x+1-\mu)^2+y^2)^{3/2}} \end{pmatrix} \quad (27)$$

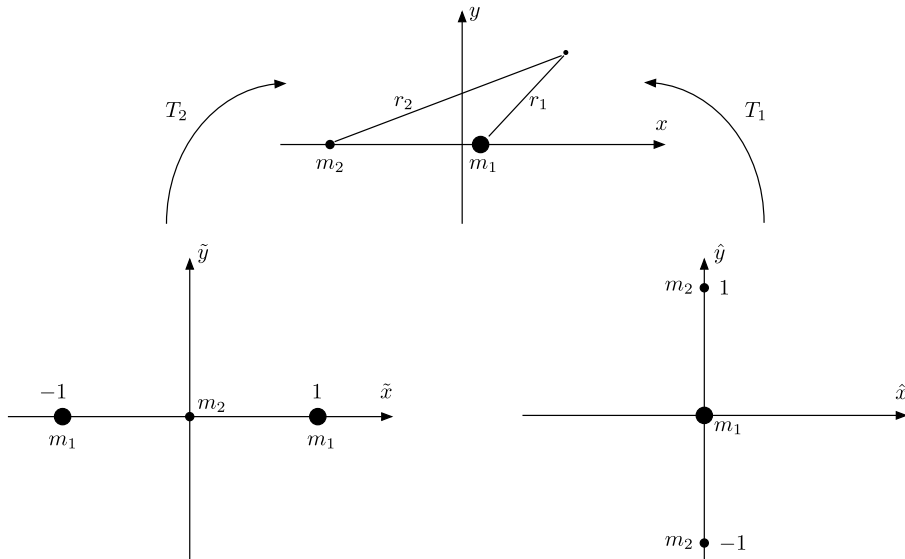


Figure 2: Three coordinate frames for the PCRTBP: the center top image depicts the classical PCRTBP in the rotating frame. The bottom left and right frames depict the restricted three body problem in Levi-Civita coordinates: regularization of collisions with m_2 on the left and with m_1 on the right. Observe that in these coordinates the regularized body has been moved to the origin. The Levi-Civita transformations T_1 and T_2 provide double covers of the original system, so that in the regularized frames there are singularities at the two copies of the remaining body.

is equivalent to the second order system given in (26). Note that

$$\|f(x, p, y, q)\| \rightarrow \infty \quad \text{as either} \quad (x, y) \rightarrow (\mu, 0) \quad \text{or} \quad (x, y) \rightarrow (\mu - 1, 0).$$

Let $\mathbf{x} = (x, p, y, q)$ denote the coordinates in U and denote by $\phi(\mathbf{x}, t)$ the flow generated by f on U . The system (27) has an integral of motion $E: U \rightarrow \mathbb{R}$ given by

$$E(\mathbf{x}) = -p^2 - q^2 + 2\Omega(x, y), \quad (28)$$

which is referred to as the Jacobi integral.

We are interested in orbits with initial conditions $\mathbf{x} \in U$ with the property that their positions limit to either $m_1 := (\mu, 0)$ or $m_2 := (\mu - 1, 0)$ in finite time. Such orbits, which reach a singularity of the vector field f in finite time, are called collisions. It has long been known that if we fix our attention to a specific level set of the Jacobi integral for some fixed $c \in \mathbb{R}$, then it is possible to make a change of coordinates which “removes” or regularizes the singularities. This idea is reviewed in the next sections.

3.1. Regularization of collisions with m_1

To regularize a collision with m_1 , define the complex variables $z = x + iy$, and the new “regularized” variables $\hat{z} = \hat{x} + i\hat{y}$, related to z by the transformation

$$\hat{z}^2 = z - \mu.$$

One also rescales time in the regularized coordinates with the rescaled time \hat{t} related to the original time t by the formula

$$\frac{dt}{d\hat{t}} = 4|\hat{z}|^2.$$

Let $U_1 \in \mathbb{R}^4$ denote the open set

$$U_1 = \{\hat{\mathbf{x}} = (\hat{x}, \hat{p}, \hat{y}, \hat{q}) \in \mathbb{R}^4 : (\hat{x}, \hat{y}) \notin \{(0, -1), (0, 1)\}\}.$$

This set will be the domain of the regularized vector field which allows us to “flow through” collisions with m_1 but not with m_2 .

A lengthy calculation (see [3]), applying the change of coordinates and time rescaling just described to the vector field f defined in Equation (27) leads to the regularized Levi-Civita vector field $f_1^c: U_1 \rightarrow \mathbb{R}^4$ with the ODE $\hat{\mathbf{x}}' = f_1^c(\hat{\mathbf{x}})$ given by

$$\begin{aligned} \hat{x}' &= \hat{p}, \\ \hat{p}' &= 8(\hat{x}^2 + \hat{y}^2)\hat{q} + 12\hat{x}(\hat{x}^2 + \hat{y}^2)^2 + 16\mu\hat{x}^3 + 4(\mu - c)\hat{x} \\ &\quad + \frac{8\mu(\hat{x}^3 - 3\hat{x}\hat{y}^2 + \hat{x})}{((\hat{x}^2 + \hat{y}^2)^2 + 1 + 2(\hat{x}^2 - \hat{y}^2))^{3/2}}, \\ \hat{y}' &= \hat{q}, \\ \hat{q}' &= -8(\hat{x}^2 + \hat{y}^2)\hat{p} + 12\hat{y}(\hat{x}^2 + \hat{y}^2)^2 - 16\mu\hat{y}^3 + 4(\mu - c)\hat{y} \\ &\quad + \frac{8\mu(-\hat{y}^3 + 3\hat{x}^2\hat{y} + \hat{y})}{((\hat{x}^2 + \hat{y}^2)^2 + 1 + 2(\hat{x}^2 - \hat{y}^2))^{3/2}}, \end{aligned} \tag{29}$$

where the parameter c in the above ODE is $c = E(x, p, y, q)$. The main observation is that the regularized vector field is well defined at the origin $(\hat{x}, \hat{y}) = (0, 0)$, and that the origin maps to the collision with m_1 when we invert the Levi-Civita coordinate transformation.

Let $\psi_1^c(\hat{\mathbf{x}}, \hat{t})$ denote the flow generated by f_1^c . The flow conserves the first integral $E_1^c: U_1 \rightarrow \mathbb{R}$ given by

$$\begin{aligned} E_1^c(\hat{\mathbf{x}}) &= -\hat{q}^2 - \hat{p}^2 + 4(\hat{x}^2 + \hat{y}^2)^3 + 8\mu(\hat{x}^4 - \hat{y}^4) + 4(\mu - c)(\hat{x}^2 + \hat{y}^2) \\ &\quad + 8(1 - \mu) + 8\mu \frac{(\hat{x}^2 + \hat{y}^2)}{\sqrt{(\hat{x}^2 + \hat{y}^2)^2 + 1 + 2(\hat{x}^2 - \hat{y}^2)}}. \end{aligned} \tag{30}$$

Note that the parameter c appears both in the formulae for f_1^c and E_1^c . We write ψ_1^c to stress that the flow depends explicitly on the choice of c . We choose $c \in \mathbb{R}$ and then, after regularization, have new coordinates which allow us to study collisions only in the level set

$$M := \{\mathbf{x} \in U : E(\mathbf{x}) = c\}. \tag{31}$$

We define the linear subspace $\mathcal{C}_1 \subset \mathbb{R}^4$ by

$$\mathcal{C}_1 = \{(\hat{x}, \hat{p}, \hat{y}, \hat{q}) \in \mathbb{R}^4 \mid \hat{x} = \hat{y} = 0\},$$

The change of coordinates between the two coordinate systems is given by the transform $T_1: U_1 \setminus \mathcal{C}_1 \rightarrow U$,

$$\mathbf{x} = T_1(\hat{\mathbf{x}}) := \begin{pmatrix} \hat{x}^2 - \hat{y}^2 + \mu \\ \frac{\hat{x}\hat{p} - \hat{y}\hat{q}}{2(\hat{x}^2 + \hat{y}^2)} \\ 2\hat{x}\hat{y} \\ \frac{\hat{y}\hat{p} + \hat{x}\hat{q}}{2(\hat{x}^2 + \hat{y}^2)} \end{pmatrix}, \tag{32}$$

and is a local diffeomorphism on $U_1 \setminus \mathcal{C}_1$. The following theorem collects results from [3], and relates the dynamics of the original and the regularized systems.

Theorem 19. *Let c be the fixed parameter determining the level set M in Equation (31). Assume that $\mathbf{x}_0 \in U$ satisfies $E(\mathbf{x}_0) = c$, and assume that $\hat{\mathbf{x}}_0 \in U_1 \setminus \mathcal{C}_1$ is such that $\mathbf{x}_0 = T_1(\hat{\mathbf{x}}_0)$. Then the curve*

$$\gamma(s) := T_1(\psi_1^c(\hat{\mathbf{x}}_0, s))$$

parameterizes the following possible solutions of the PCRTBP in M :

1. *If for every $\hat{t} \in [-\hat{T}, \hat{T}]$ we have $\psi_1^c(\hat{\mathbf{x}}_0, \hat{t}) \in U_1 \setminus \mathcal{C}_1$, then $\gamma(s)$, for $s \in [-\hat{T}, \hat{T}]$ lies on a trajectory of the PCRTBP which avoids collisions. Moreover, the time t in the original coordinates that corresponds to the time $\hat{t} \in [-\hat{T}, \hat{T}]$ in the regularised coordinates is recovered by the integral*

$$t = 4 \int_0^{\hat{t}} (\hat{x}(s)^2 + \hat{y}(s)^2) ds, \quad (33)$$

i.e.

$$\phi(t, \mathbf{x}_0) = T_1(\psi_1^c(\hat{\mathbf{x}}_0, \hat{t})).$$

2. *If for $\hat{T} > 0$, for every $\hat{t} \in [0, \hat{T}]$ we have $\psi_1^c(\hat{\mathbf{x}}_0, \hat{t}) \in U_1 \setminus \mathcal{C}_1$ and $\psi_1^c(\hat{\mathbf{x}}_0, \hat{T}) \in \mathcal{C}_1$, then in the original coordinates the trajectory starting from \mathbf{x}_0 reaches the collision with m_1 at time $T > 0$ given by*

$$T = 4 \int_0^{\hat{T}} (\hat{x}(s)^2 + \hat{y}(s)^2) ds. \quad (34)$$

3. *If for $\hat{T} < 0$, for every $\hat{t} \in (\hat{T}, 0]$ we have $\psi_1^c(\hat{\mathbf{x}}_0, \hat{t}) \in U_1 \setminus \mathcal{C}_1$ and $\psi_1^c(\hat{\mathbf{x}}_0, \hat{T}) \in \mathcal{C}_1$, then in the original coordinates the backward trajectory starting from \mathbf{x}_0 reaches the collision with m_1 at time $T < 0$ expressed in Equation (34).*

Orbits satisfying condition 2 from Theorem 19 are collision orbits, while orbits satisfying condition 3 from Theorem 19 are called ejection orbits. From Theorem 19 we see that for regularized orbits $\psi_1^c(\hat{\mathbf{x}}_0, \hat{t})$ to have a physical meaning in the original coordinates we need to choose $c = E(T_1(\hat{\mathbf{x}}_0))$ for the regularization energy. The following lemma, whose proof is a standard calculation (see [3]), addresses this choice.

Lemma 20. *For every $\hat{\mathbf{x}} \in U_1$, we have*

$$E(T_1(\hat{\mathbf{x}})) = c \quad \text{if and only if} \quad E_1^c(\hat{\mathbf{x}}) = 0. \quad (35)$$

The following corollary of Lemma 20 is a consequence of evaluating the expression for the energy at zero when the positions are zero.

Corollary 21. *If we consider $\hat{\mathbf{x}} = (\hat{x}, \hat{p}, \hat{y}, \hat{q})$ with $\hat{x} = \hat{y} = 0$, which corresponds to a collision with m_1 , then from $E_1^c(\hat{\mathbf{x}}) = 0$ we see that for a trajectory $\psi_1^c(\hat{\mathbf{x}}, \hat{t})$ starting from a collision point $\hat{\mathbf{x}} = (0, \hat{p}, 0, \hat{q})$ to have a physical meaning in the original coordinates it is necessary and sufficient that*

$$\hat{q}^2 + \hat{p}^2 = 8(1 - \mu). \quad (36)$$

Definition 22. We refer to

$$\{\psi_1^c(\hat{\mathbf{x}}, \hat{t}) : \hat{q}^2 + \hat{p}^2 = 8(1 - \mu), \hat{t} \geq 0 \text{ and } \psi_1^c(\hat{\mathbf{x}}, [0, \hat{t}]) \cap \mathcal{C}_1 = \emptyset\}$$

as the ejection manifold from m_1 , and

$$\{\psi_1^c(\hat{\mathbf{x}}, \hat{t}) : \hat{q}^2 + \hat{p}^2 = 8(1 - \mu), \hat{t} \leq 0 \text{ and } \psi_1^c(\hat{\mathbf{x}}, [\hat{t}, 0]) \cap \mathcal{C}_1 = \emptyset\}$$

as the collision manifold to m_1 .

Note that both the collision and the ejection manifolds depend on the choice of c . That is, we have a family of collision/ejection manifolds, parameterized by the Jacobi constant c . For a fixed c the collision manifold, when viewed in the original coordinates, consists of points with energy c , whose forward trajectory reaches the collision with m_1 . Similarly, for fixed c , the ejection manifold, in the original coordinates, consists of points with energy c whose backward trajectory collide with m_1 . Thus, the circle defined in Corollary 21 is a sort of “fundamental domain” for ejections/collisions to m_1 with energy c .

3.2. Regularization of collisions with m_2

To regularize at the second primary, we define the coordinates $\tilde{z} = \tilde{x} + i\tilde{y}$ through $\tilde{z}^2 = z + 1 - \mu$ and consider the time rescaling $dt/d\tilde{t} = 4|\tilde{z}|^2$. As in the previous section, define

$$\begin{aligned} U_2 &:= \{\tilde{\mathbf{x}} = (\tilde{x}, \tilde{p}, \tilde{y}, \tilde{q}) \in \mathbb{R}^4 \mid (\tilde{x}, \tilde{y}) \notin \{(-1, 0), (1, 0)\}\}, \\ \mathcal{C}_2 &:= \{\tilde{\mathbf{x}} = (\tilde{x}, \tilde{p}, \tilde{y}, \tilde{q}) \in \mathbb{R}^4 \mid \tilde{x} = \tilde{y} = 0\}, \end{aligned}$$

so that U_2 consists of points in the regularized coordinates which do not collide with m_1 , and \mathcal{C}_2 consists of points which collide with m_2 .

The regularized Levi-Civita vector field $f_2^c : U_2 \rightarrow \mathbb{R}^4$ with the ODE $\tilde{\mathbf{x}}' = f_2^c(\tilde{\mathbf{x}})$ is of the form (see [3])

$$\begin{aligned} \tilde{x}' &= \tilde{p}, \\ \tilde{p}' &= 8(\tilde{x}^2 + \tilde{y}^2)\tilde{q} + 12\tilde{x}(\tilde{x}^2 + \tilde{y}^2)^2 - 16(1 - \mu)\tilde{x}^3 + 4((1 - \mu) - c)\tilde{x} \\ &\quad + \frac{8(1 - \mu)(-\tilde{x}^3 + 3\tilde{x}\tilde{y}^2 + \tilde{x})}{((\tilde{x}^2 + \tilde{y}^2)^2 + 1 + 2(\tilde{y}^2 - \tilde{x}^2))^{3/2}}, \\ \tilde{y}' &= \tilde{q}, \\ \tilde{q}' &= -8(\tilde{y}^2 + \tilde{x}^2)\tilde{p} + 12\tilde{y}(\tilde{x}^2 + \tilde{y}^2)^2 + 16(1 - \mu)\tilde{y}^3 + 4((1 - \mu) - c)\tilde{y} \\ &\quad + \frac{8(1 - \mu)(\tilde{y}^3 - 3\tilde{x}^2\tilde{y} + \tilde{y})}{((\tilde{x}^2 + \tilde{y}^2)^2 + 1 + 2(\tilde{y}^2 - \tilde{x}^2))^{3/2}}, \end{aligned} \tag{37}$$

with the integral of motion

$$\begin{aligned} E_2^c(\tilde{\mathbf{x}}) &= -\tilde{p}^2 - \tilde{q}^2 + 4(\tilde{x}^2 + \tilde{y}^2)^3 + 8(1 - \mu)(\tilde{y}^4 - \tilde{x}^4) + 4((1 - \mu) - c)(\tilde{x}^2 + \tilde{y}^2) \\ &\quad + 8(1 - \mu)\frac{\tilde{x}^2 + \tilde{y}^2}{\sqrt{(\tilde{x}^2 + \tilde{y}^2)^2 + 1 + 2(\tilde{y}^2 - \tilde{x}^2)}} + 8\mu. \end{aligned} \tag{38}$$

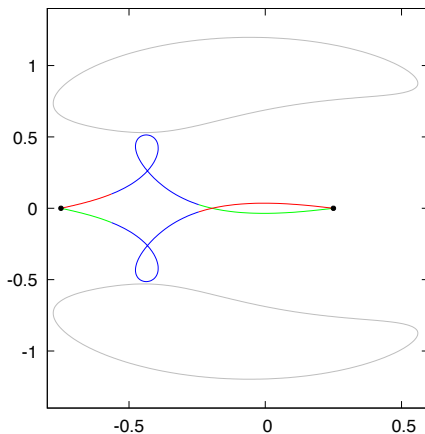


Figure 3: Ejection collision orbits in the PCRTBP when $\mu = 1/4$ and $C = 3.2$. The grey curves at the top and bottom of the figure illustrate the zero velocity curves, i.e. the boundaries of the prohibited Hill's regions, for this value of C . The black dots at $x = \mu$ and $x = -1 + \mu$ depict the locations of the primary bodies. The curves in the middle of the figure represent two ejection-collision orbits: m_2 to m_1 (bottom) and m_1 to m_2 (top). (Recall that m_2 is on the left and m_1 on the right; compare with Figure 2.) These orbits are computed by numerically locating an approximate zero of the function defined in Equation (44). The blue portion of the orbit is in the original coordinates, while green and red are on the ejection and collision manifolds in regularized coordinates, respectively. The curves are plotted by changing all points back to the original coordinates.

We write $\psi_2^c(\tilde{\mathbf{x}}, \tilde{t})$ for the flow induced by (37).

The change of coordinates from the regularized coordinates $\tilde{\mathbf{x}}$ to the original coordinates \mathbf{x} is given by $T_2 : U_2 \setminus \mathcal{C}_2 \rightarrow \mathbb{R}^4$ of the form

$$\mathbf{x} = T_2(\tilde{\mathbf{x}}) = \begin{pmatrix} \tilde{x}^2 - \tilde{y}^2 + \mu - 1 \\ \frac{\tilde{x}\tilde{p} - \tilde{y}\tilde{q}}{2(\tilde{x}^2 + \tilde{y}^2)} \\ 2\tilde{x}\tilde{y} \\ \frac{\tilde{y}\tilde{p} + \tilde{x}\tilde{q}}{2(\tilde{x}^2 + \tilde{y}^2)} \end{pmatrix}. \quad (39)$$

A theorem analogous to Theorem 19 characterizes solution curves in the two coordinate systems and the collisions with the second primary m_2 . Also, analogously to Lemma 20 and Corollary 21 for every $\tilde{\mathbf{x}} \in U_2$ we have

$$E(T_2(\tilde{\mathbf{x}})) = c \quad \text{if and only if} \quad E_2^c(\tilde{\mathbf{x}}) = 0, \quad (40)$$

and a trajectory $\psi_2^c(\tilde{\mathbf{x}}, \tilde{t})$ starting from a collision point $\tilde{\mathbf{x}} = (0, \tilde{p}, 0, \tilde{q})$ with m_2 has physical meaning in the original coordinates if and only if

$$\tilde{q}^2 + \tilde{p}^2 = 8\mu. \quad (41)$$

We introduce the notions of the ejection and collision manifolds for m_2 analogously to Definition 22.

4. Ejection-collision orbits

We now define a level set multiple shooting operator whose zeros correspond to transverse ejection-collision orbits from the body m_k to the body m_l for $k, l \in \{1, 2\}$ in the PCRTBP. Two such orbits in the PCRTBP are illustrated in Figure 3.

Note that the PCRTBP has the form discussed in Example 16, so that a dissipative unfolding is given by the one parameter family of ODEs

$$f_\alpha(x, p, y, q) = f(x, p, y, q) + \alpha(0, p, 0, q), \quad (42)$$

where f is as defined in Equation (27). Let $\phi_\alpha(\mathbf{x}, t)$ denote the flow generated by the the vector field of Equation (42). For $c \in \mathbb{R}$ consider the fixed energy level set M . Then α is an unfolding parameter for the mapping

$$R_{\tau, \alpha}(\mathbf{x}) = \phi_\alpha(\mathbf{x}, \tau)$$

from M to M . (Here $R_{\tau, \alpha} : \mathbb{R}^4 \rightarrow \mathbb{R}^4$ for fixed $\alpha, \tau \in \mathbb{R}$.)

Define the functions $P_i : \mathbb{R} \rightarrow \mathbb{R}^4$ for $i = 1, 2$ by

$$P_i(\theta) := \begin{cases} (0, \sqrt{8(1-\mu)} \cos(\theta), 0, \sqrt{8(1-\mu)} \sin(\theta)) & \text{for } i = 1, \\ (0, \sqrt{8\mu} \cos(\theta), 0, \sqrt{8\mu} \sin(\theta)) & \text{for } i = 2. \end{cases} \quad (43)$$

By Equations (36) and (41) the function $P_i(\theta)$ parameterizes the collision set for the primary m_i , with $i = 1, 2$. Fix $k, l \in \{1, 2\}$ and consider level sets $M_1, \dots, M_6 \subset \mathbb{R}^4$ defined by

$$\begin{aligned} M_1 &= M_2 = \{E_k^c = 0\}, \\ M_3 &= M_4 = \{E = c\}, \\ M_5 &= M_6 = \{E_l^c = 0\}. \end{aligned}$$

Choose $s > 0$, and for $i = 1, 2$ recall the definition of the coordinate transformations $T_i : U_i \setminus \mathcal{C}_i \rightarrow \mathbb{R}^4$ defined in Equations (32) and (39). Taking the maps $R_{\tau, \alpha}^1, \dots, R_{\tau, \alpha}^5 : \mathbb{R}^4 \rightarrow \mathbb{R}^4$ as

$$\begin{aligned} R_{\tau, \alpha}^1(x_1) &= \psi_k^c(x_1, s), \\ R_{\tau, \alpha}^2(x_2) &= T_k(x_2), \\ R_{\tau, \alpha}^3(x_3) &= \phi_\alpha(x_3, \tau), \\ R_{\tau, \alpha}^4(x_4) &= T_l^{-1}(x_4), \\ R_{\tau, \alpha}^5(x_5) &= \psi_l^c(x_5, s), \end{aligned}$$

we let

$$F : \underbrace{\mathbb{R} \times \mathbb{R}^4 \times \dots \times \mathbb{R}^4}_{5 \text{ copies}} \times \mathbb{R} \times \mathbb{R} \times \mathbb{R} \rightarrow \underbrace{\mathbb{R}^4 \times \dots \times \mathbb{R}^4}_{6 \text{ copies}}$$

be defined as

$$F(x_0, x_1, \dots, x_5, x_6, \tau, \alpha) := \begin{pmatrix} P_k(x_0) - x_1 \\ R_{\alpha, \tau}^1(x_1) - x_2 \\ R_{\alpha, \tau}^2(x_2) - x_3 \\ R_{\alpha, \tau}^3(x_3) - x_4 \\ R_{\alpha, \tau}^4(x_4) - x_5 \\ R_{\alpha, \tau}^5(x_5) - P_l(x_6) \end{pmatrix}, \quad (44)$$

where $x_0, x_6, \tau, \alpha \in \mathbb{R}$ and $x_1, \dots, x_5 \in \mathbb{R}^4$. We also write (x_k, p_k, y_k, q_k) and (x_l, p_l, y_l, q_l) to denote the regularized coordinates given by the coordinate transformations T_k and T_l , respectively.

Lemma 23. *Let $\mathbf{x}^* = (x_0^*, \dots, x_6^*)$ and $\tau^* > 0$. If*

$$DF(\mathbf{x}^*, \tau^*, 0)$$

is an isomorphism and

$$F(\mathbf{x}^*, \tau^*, 0) = 0,$$

then the orbit of the point x_3^ is ejected from the primary body m_k and collides with the primary body m_l . (The same is true of the orbit of the point x_4^* .) Moreover, intersection of the collision and ejection manifolds is transversal on the energy level $\{E = c\}$ and the time from the ejection to the collision is*

$$\tau^* + 4 \int_0^s \|\pi_{x_k, y_k} \psi_k^c(x_1^*, u)\|^2 du + 4 \int_0^s \|\pi_{x_l, y_l} \psi_l^c(x_5^*, u)\|^2 du. \quad (45)$$

(Above we use the Euclidean norm.)

Proof. We have $d_0 = d_6 = k = 1$ and $d = 4$, so the condition in Equation (14) is satisfied. We now show that α is an unfolding parameter for $R_{\tau, \alpha} = R_{\tau, \alpha}^5 \circ \dots \circ R_{\tau, \alpha}^1$. Since E_i^c is an integral of motion for the flow ψ_i^c , for $i = 1, 2$, we see that

$$\begin{aligned} x_1 \in M_1 = \{E_k^c = 0\} & \quad \text{if and only if} & \quad R_{\tau, \alpha}^1(x_1) = \psi_k^c(x_1, s) \in M_2 = \{E_k^c = 0\}, \\ x_5 \in M_5 = \{E_l^c = 0\} & \quad \text{if and only if} & \quad R_{\tau, \alpha}^5(x_5) = \psi_l^c(x_5, s) \in M_6 = \{E_l^c = 0\}. \end{aligned}$$

Also, by Equations (35) and (40) we see that

$$\begin{aligned} x_2 \in M_2 = \{E_k^c = 0\} & \quad \text{if and only if} & \quad R_{\tau, \alpha}^2(x_2) = T_k(x_2) \in M_3 = \{E = c\}, \\ x_4 \in M_4 = \{E = c\} & \quad \text{if and only if} & \quad R_{\tau, \alpha}^4(x_2) = T_l^{-1}(x_4) \in M_5 = \{E_l^c = 0\}. \end{aligned}$$

Moreover α is an unfolding parameter for the PCRTBP, and hence for

$$R_{\tau, \alpha}^3(x_3) = \phi_\alpha(x_3, \tau).$$

Note that for $i = 1, 2, 4, 5$, the maps $R_{\tau, \alpha}^i$ takes the level sets M_i into the level set M_{i+1} and this does not depend on the choice of α . Then, since α is an unfolding parameter for $R_{\tau, \alpha}^3$, it follows directly from Definition 13 that α is an unfolding parameter for $R_{\tau, \alpha} = R_{\tau, \alpha}^5 \circ \dots \circ R_{\tau, \alpha}^1$.

By applying Lemma 18 to

$$\tilde{F}(x_0, x_6, \tau, \alpha) := R_{\tau, \alpha}(P_k(x_0)) - P_l(x_6)$$

we obtain that $D\tilde{F}(x_0^*, x_6^*, \tau^*, 0)$ is an isomorphism and that $\tilde{F}(x_0^*, x_6^*, \tau^*, 0) = 0$. Since

$$\tilde{F}(x_0^*, x_6^*, \tau^*, 0) = \psi_l^c(T_l^{-1}(\phi(T_k(\psi_k^c(P_k(x_0^*), s)), \tau^*)), s) - P_l(x_6^*),$$

we see that, by Theorem 19 (and its mirror counterpart for the collision with m_2) we have an orbit originating at the point $P_k(x_0^*)$ on the collision set for m_k , and terminating at the point $P_l(x_6^*)$ on the collision set for m_l . The transversality of the intersection between the ejection manifold of m_k and the collision manifold of m_l follows from Theorem 15. The time between collisions in Equation (45) follows from Equation (34). ■

Remark 24 (Additional shooting steps). We remark that in practice, computing accurate enclosures of flow maps requires shortening the time step. Consider for example the third and fourth component of F as defined in Equation (44), and suppose that time step of length τ/N is desired. By the properties of the flow map, solving the sub-system of equations

$$\begin{aligned} R_{\alpha,\tau}^3(x_3) - x_4 &= \phi_\alpha(x_3, \tau) - x_4 = 0 \\ R_{\alpha,\tau}^4(x_4) - x_5 &= T_l^{-1}(x_4) - x_5 = 0 \end{aligned} \tag{46}$$

is equivalent to solving

$$\begin{aligned} \phi_\alpha(x_3, \tau/N) - y_1 &= 0 \\ \phi_\alpha(y_1, \tau/N) - y_2 &= 0 \\ &\vdots \\ \phi_\alpha(y_{N-2}, \tau/N) - y_{N-1} &= 0 \\ \phi_\alpha(y_{N-1}, \tau/N) - x_4 &= 0 \\ T_l^{-1}(x_4) - x_5 &= 0, \end{aligned}$$

and we can append these new variables and components to the map F defined in Equation (44) without changing the zeros of the operator. Moreover, by Lemma 18 the transversality result for the operator is not changed by the addition of additional steps. Indeed, by the same reasoning we can (and do) add intermediate shooting steps in the regularized coordinates to reduce the time steps to any desired tolerance.

5. Connections between collisions and libration points L_4, L_5

For each value of $\mu \in (0, 1/2]$, the PCRTBP has exactly five equilibrium solutions. For traditional reasons, these are referred to as libration points of the PCRTBP. Three of these are collinear with the primary bodies, and lie on the x -axis. These are referred to as L_1, L_2 and L_3 , and they correspond to the co-linear relative equilibrium solutions discovered by Euler. The remaining two libration points are located at the third vertex of the equilateral triangles whose other two vertices are the primary and secondary bodies. These are referred to as L_4 and L_5 , and correspond to the equilateral triangle solutions of Lagrange. Figure 4 illustrates the locations of the libration points in the phase space.

For all values of the mass ratio, the collinear libration points have saddle \times center stability. The center manifolds give rise to important families of periodic orbits known as Lyapunov families. The stability of L_4 and L_5 depend on the mass ratio μ . For

$$0 < \mu < \mu_* \approx 0.04,$$

where the exact value is $\mu_* = 2/(25 + \sqrt{621})$, the triangular libration points have center \times center stability. That is, they are stable in the the sense of Hamiltonian systems and exhibit the full “zoo” of nearby KAM objects.

When $\mu > \mu_*$, the triangular libration points L_4 and L_5 have saddle-focus stability. That is, they have a complex conjugate pair of stable and a complex conjugate pair of unstable eigenvalues. The four eigenvalues then have the form

$$\lambda = \pm\alpha \pm i\beta,$$

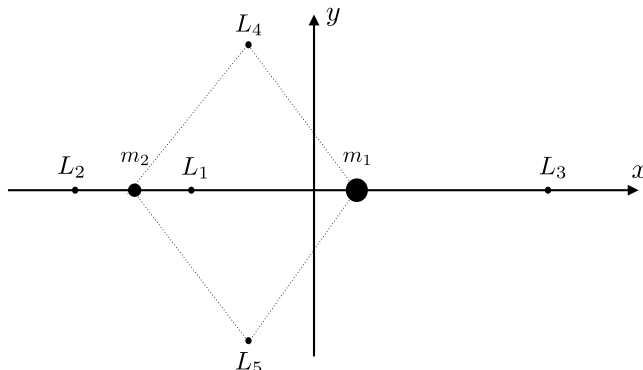


Figure 4: The three collinear libration points $L_{1,2,3}$ and the equilateral triangle libration points $L_{4,5}$, relative to the positions of the primary masses m_1 and m_2 .

for some $\alpha, \beta > 0$. In this case, each libration point has an attached two dimensional stable and two dimensional unstable manifold. Since these two dimensional manifolds live in the three dimensional energy level set of $L_{4,5}$, there exists the possibility that they intersect the two dimensional collision or ejection manifolds of the primaries transversely. It is also possible that the stable/unstable manifolds of $L_{4,5}$ intersect one other transversely giving rise to homoclinic or heteroclinic connecting orbits.

In fact, in this paper we prove that both of these phenomena occur and in this section we discuss our method for proving the existence of intersections between a stable/unstable manifold of $L_{4,5}$, and an ejection/collision manifold of a primary body. Any point of intersection between these manifolds gives rise to an orbit which is asymptotic to L_4 , but which collides or is ejected from one of the massive bodies. Two such orbits are illustrated in Figure 5.

Let $\bar{B} \subset \mathbb{R}^2$ denote a closed ball with radius 1. Assume that

$$w_j^\kappa : \bar{B} \rightarrow \mathbb{R}^4 \quad \text{for } j \in \{4, 5\} \text{ and } \kappa \in \{u, s\},$$

parameterize the two dimensional local stable/unstable manifolds of L_j . We assume that the charts are normalized so that $w_j^\kappa(0) = L_j$. Then

$$w_j^\kappa(\bar{B}) = W_{\text{loc}}^\kappa(L_j) \quad \text{for } j \in \{4, 5\}, \kappa \in \{u, s\}.$$

Define the functions

$$P_j^\kappa : \mathbb{R} \rightarrow \mathbb{R}^4 \quad \text{for } j \in \{4, 5\} \text{ and } \kappa \in \{u, s\},$$

by

$$P_j^\kappa(\theta) := w_j^\kappa(\cos \theta, \sin \theta). \quad (47)$$

For $i \in \{1, 2\}$ consider P_i as defined in Equation (43).

For

$$\mathbf{x} = (x_0, x_1, x_2, x_3, x_4) \in \mathbb{R}^{14},$$

where $x_0, x_4 \in \mathbb{R}$, $x_1, x_2, x_3 \in \mathbb{R}^4$, and $j \in \{4, 5\}$ we define

$$F_{i,j}^u, F_{i,j}^s : \mathbb{R}^{16} \rightarrow \mathbb{R}^{16},$$

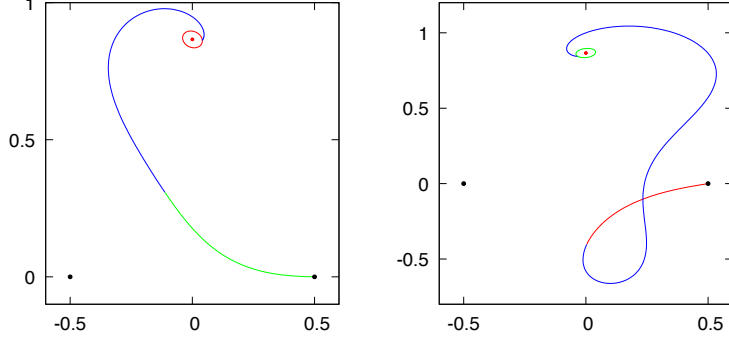


Figure 5: Libration-to-collision and ejection-to-libration orbits for $\mu = 1/2$ and $c = 3$ (which is the L_4 value of the Jacobi constant in the equal mass problem). The left frame illustrates an ejection to L_4 orbit, and the right frame an L_4 to collision. In each frame m_1 is depicted as a black dot and L_4 as a red dot. The boundary of a parameterized local unstable manifold for L_4 is depicted as the red circle; stable boundary the green circle. The orbits are found by computing an approximate zero of the map defined in Equation (48). The green portion of the left, and red portion of the right curves are computed in regularized coordinates for the body m_1 . These points are transformed back to the original coordinates for the plot.

by the formulas

$$F_{i,j}^u(\mathbf{x}, \tau, \alpha) = \begin{pmatrix} P_j^u(x_0) - x_1 \\ \phi_\alpha(x_1, \tau) - x_2 \\ T_i^{-1}(x_2) - x_3 \\ \psi_i^{c_j}(x_3, s) - P_i(x_4) \end{pmatrix}, \quad F_{i,j}^s(\mathbf{x}, \tau, \alpha) = \begin{pmatrix} P_i(x_0) - x_1 \\ \psi_i^{c_j}(x_1, s) - x_2 \\ T_i(x_2) - x_3 \\ \phi_\alpha(x_3, \tau) - P_j^s(x_4) \end{pmatrix}. \quad (48)$$

Here $\tau, \alpha \in \mathbb{R}$ and the constant c_j in $\psi_i^{c_j}$ is chosen as $c_j = E(L_j)$.

Zeros of the operator $F_{i,j}^u$ correspond to intersections of the unstable manifold of L_j with the collision manifold of mass m_i . We also refer to this as a heteroclinic connection from L_j to m_i . Similarly, zeros of the operator $F_{i,j}^s$ correspond to intersections between the stable manifold of L_j with the ejection manifold of mass m_i . In other words, they lead to heteroclinic connections ejected from m_i and limiting to the libration point L_j in forward time. This is expressed formally in the following lemma.

Lemma 25. Fix $i \in \{1, 2\}$, $j \in \{4, 5\}$, and $\kappa \in \{u, s\}$. Suppose there exists $\mathbf{x}^* = (x_0^*, x_1^*, x_2^*, x_3^*, x_4^*) \in \mathbb{R}^{14}$ and $\tau^* > 0$ satisfying

$$F_{i,j}^\kappa(\mathbf{x}^*, \tau^*, 0) = 0,$$

and such that

$$DF_{i,j}^\kappa(\mathbf{x}^*, \tau^*, 0)$$

is an isomorphism. Then we have the following two cases.

1. If $\kappa = u$, then the orbit of x_1^* is heteroclinic from the libration point L_j to collision with m_i and the intersection of $W^u(L_j)$ with the collision manifold of m_i is transverse with respect to the energy level $\{E = c_j\}$.

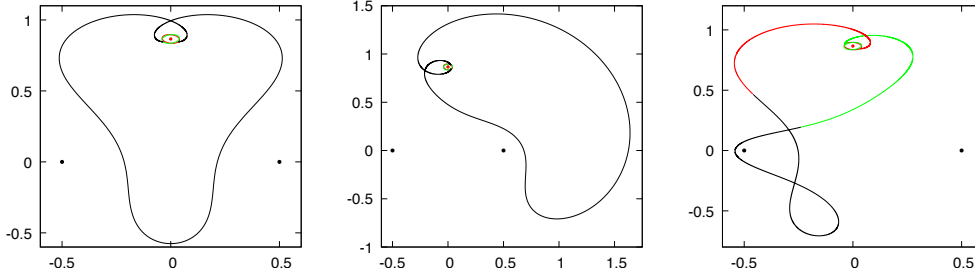


Figure 6: Transverse homoclinic orbits at L_4 for $\mu = 1/2$ in the $C = 3$ energy level. Each orbit traverses the illustrated curves in a clockwise fashion. The left and center orbits were known to Stromgren and Szebeheley. The center and right orbits possess no symmetry, and the orbit on the right passes close to collision with m_2 . Each orbit is found by approximately computing a zero of the map defined in Equation (49). The left and center orbits are computed in only the standard coordinate system. The orbit on the right is computed by changing to regularized coordinates for the middle third of the flight.

2. If $\kappa = s$, then the orbit of x_3^* is heteroclinic from the libration point L_j to ejection with m_i and the intersection of $W^s(L_j)$ with the ejection manifold of m_i is transverse with respect to the energy level $\{E = c_j\}$.

Proof. The proof follows from an argument similar to the proof of Lemma 23. ■

By a small modification of the operator just defined, we can study orbits homoclinic or heteroclinic to the libration points as well. Such orbits arise as intersections of the stable/unstable manifolds of the libration points, and lead naturally to two point BVPs. Three such orbits, homoclinic to L_4 in the PCRTBP, are illustrated in Figure 6.

Note that homoclinic/heteroclinic connections between equilibrium solutions do not require changing to regularized coordinates as such orbits exist for all forward and backward time and cannot have any collisions. While this claim is mathematically correct, any homoclinic/heteroclinic orbit which passes sufficiently close to a collision with m_i for $i \in \{1, 2\}$ becomes difficult to continue numerically. Consequently, these orbits may still be difficult or impossible to validate via computer assisted proof. In this case regularization techniques are an asset even when studying orbits which pass near a collision. The left and center homoclinic orbits in Figure 6 for example are computed entirely in the usual PCRTBP coordinates, while the right orbit was computed using both coordinate systems. With this in mind we express the homoclinic/heteroclinic problem in the framework set up in the previous sections.

Let $P_j^c : \mathbb{R} \rightarrow \mathbb{R}^4$, for $j \in \{4, 5\}$ be the functions defined in Equation (47) and consider

$$\mathbf{x} = (x_0, \dots, x_6) \in \mathbb{R}^{22},$$

where $x_0, x_6 \in \mathbb{R}$ and $x_1, \dots, x_5 \in \mathbb{R}^4$, and fix $s_1, s_2 > 0$. Let

$$F_{i,j,k} : \mathbb{R}^{24} \rightarrow \mathbb{R}^{24}, \quad \text{for } j, k \in \{4, 5\}, i \in \{1, 2\},$$

be defined as

$$F_{i,j,k}(\mathbf{x}, \tau, \alpha) := \begin{pmatrix} P_j^u(x_0) - x_1 \\ \phi_\alpha(x_1, \tau) - x_2 \\ T_i^{-1}(x_2) - x_3 \\ \psi_i^{c_j}(x_3, s_1) - x_4 \\ T_i(x_4) - x_5 \\ \phi_\alpha(x_5, s_2) - P_k^s(x_6) \end{pmatrix}. \quad (49)$$

One can formulate an analogous result to the Lemmas 23 and 25, so that

$$F_{i,j,k}(\mathbf{x}^*, \tau^*, 0) = 0,$$

together with $DF_{i,j,k}(\mathbf{x}^*, \tau^*, 0)$ an isomorphism implies that the manifolds $W^u(L_j)$ and $W^s(L_k)$ intersect transversally.

Again, the advantage of solving $F_{i,j,k} = 0$ over parallel shooting in the original coordinates is that one can establish the existence of connections which pass arbitrarily close to a collision m_1 and/or m_2 . Indeed, the operator defined in Equation (49) can be generalized to study homoclinic orbits which make any finite number of flybys of the primaries in any order before returning to $L_{4,5}$ by making additional changes of variables to regularized coordinates every time the orbit passes near collision.

6. Symmetric periodic orbits passing through collision

In this section we show that our method applies to the study of families of periodic orbits which pass through a collision. By this we mean the following. We will prove the existence of a family of orbits parameterized by the value of the Jacobi constant on an interval. As in the introduction, we refer to this as a tube of periodic orbits. For all values in the interval except one, the intersection of the energy level set with the tube is a periodic orbit. For a single isolated value of the energy the intersection of the energy level set with the tube is an ejection-collision orbit involving m_1 . The situation is depicted in Figure 7.

To establish such a family of periodic orbits we make use of the time reversing symmetry of the PCRTBP. Recall that for

$$S(x, p, y, q) := (x, -p, -y, q)$$

and for the flow $\phi(\mathbf{x}, t)$ of the PCRTBP we have that

$$S(\phi(\mathbf{x}, t)) = \phi(S(\mathbf{x}), -t). \quad (50)$$

Let us introduce the notation \mathcal{S} to stand for the set of self S -symmetric points

$$\mathcal{S} := \{\mathbf{x} \in \mathbb{R}^4 : \mathbf{x} = S(\mathbf{x})\}.$$

The property in Equation (50) is used to find periodic orbits as follows. Suppose $\mathbf{x}, \mathbf{y} \in \mathcal{S}$ satisfy $\mathbf{y} = \phi(\mathbf{x}, t)$. Then by Equation (50), we have

$$\phi(\mathbf{x}, 2t) = \phi(\mathbf{y}, t) = \phi(S(\mathbf{y}), t) = S(\phi(\mathbf{y}, -t)) = S(\mathbf{x}) = \mathbf{x}, \quad (51)$$

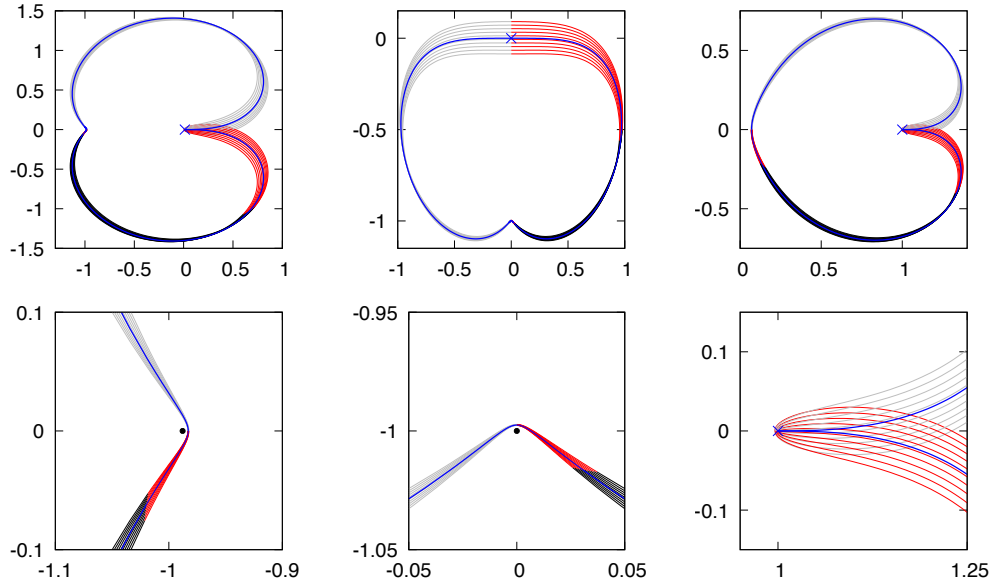


Figure 7: A family of Lyapunov periodic orbits passing through a collision. The left two figures are in the original coordinates, the middle two are in the regularised coordinates at m_1 and the right two are in regularised coordinates at m_2 . (Compare with Figure 2.) The trajectories computed in the original coordinates are in black, and the trajectories computed in the regularized coordinates are in red. The collision with m_1 is indicated by a cross. The mass m_2 is added in the closeup figures as a black dot. The operator (54) gives half of a periodic orbit in red and black. The second half, which follows from the symmetry, is depicted in grey. The plots are for the Earth-moon system.

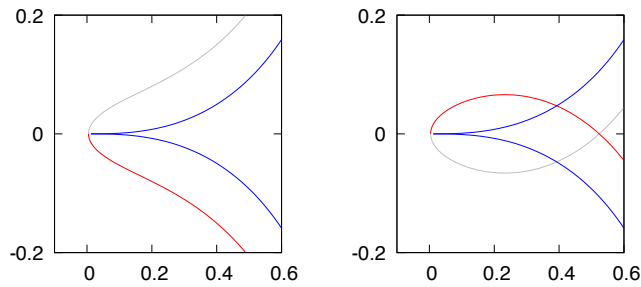


Figure 8: A closeup of a Lyapunov orbit before (left) and after (right) passing through the collision. The plot is in the original coordinates.

meaning that \mathbf{x} lies on a periodic orbit. Our strategy is then to set up a boundary value problem which shoots from \mathcal{S} to itself.

The set \mathcal{S} lies on the x -axis in the (x, y) coordinate frame. From the left plot in Figure 7 it is clear that we are interested in points on \mathcal{S} which will pass through collision with m_1 and close to the collision with m_2 . We therefore consider the set \mathcal{S} transformed to the regularized coordinates of m_1 and m_2 .

Lemma 26. *Let $\hat{\mathcal{S}}, \tilde{\mathcal{S}} \subset \mathbb{R}^4$ be defined as*

$$\begin{aligned}\hat{\mathcal{S}} &= \{(0, \hat{p}, \hat{y}, 0) : \hat{p}, \hat{y} \in \mathbb{R}\}, \\ \tilde{\mathcal{S}} &= \{(\tilde{x}, 0, 0, \tilde{q}) : \tilde{x}, \tilde{q} \in \mathbb{R}\}.\end{aligned}$$

Then $T_1(\hat{\mathcal{S}}) = \mathcal{S}$ and $T_2(\tilde{\mathcal{S}}) = \mathcal{S}$.

Proof. The proof follows directly from the definition of T_1 and T_2 . (See Equations (32) and (39).) ■

The intuition behind the choice of $\hat{\mathcal{S}}, \tilde{\mathcal{S}}$ is seen in Figure 2. From the figure we see that the set $\hat{\mathcal{S}}$ is the vertical axis $\{\hat{x} = 0\}$ and $\tilde{\mathcal{S}}$ is the horizontal axis $\{\tilde{y} = 0\}$, which join the primaries in the regularized coordinates.

To find the desired symmetric periodic orbits we fix an energy level $c \in \mathbb{R}$ and introduce an appropriate shooting operator, whose zero implies the existence of an orbit with energy c . Slightly abusing notation, let us first define two functions $\hat{p}, \tilde{q} : \mathbb{R}^2 \rightarrow \mathbb{R}$ as

$$\begin{aligned}\hat{p}(\hat{y}, c) &:= \sqrt{4\hat{y}^6 - 8\mu\hat{y}^4 + 4(\mu - c)\hat{y}^2 + \frac{8\mu\hat{y}^2}{\sqrt{\hat{y}^4 + 1 - 2\hat{y}^2}} + 8(1 - \mu)}, \\ \tilde{q}(\tilde{x}, c) &:= \sqrt{4\tilde{x}^6 - 8(1 - \mu)\tilde{x}^4 + 4((1 - \mu) - c)\tilde{x}^2 + \frac{8(1 - \mu)\tilde{x}^2}{\sqrt{\tilde{x}^4 + 1 - 2\tilde{x}^2}} + 8\mu}.\end{aligned}$$

Observe that from Equations (30) and (38) we have

$$E_1^c(0, \hat{p}(\hat{y}, c), \hat{y}, 0) = 0, \quad (52)$$

$$E_2^c(\tilde{x}, 0, 0, \tilde{q}(\tilde{x}, c)) = 0. \quad (53)$$

Next, we define $P_1^c, P_2^c : \mathbb{R} \rightarrow \mathbb{R}^4$ by

$$\begin{aligned}\hat{P}_1^c(\hat{y}) &:= (0, \hat{p}(\hat{y}, c), \hat{y}, 0), \\ \tilde{P}_2^c(\tilde{x}) &:= (\tilde{x}, 0, 0, \tilde{q}(\tilde{x}, c)),\end{aligned}$$

and note that $P_1^c(\mathbb{R}) \subset \hat{\mathcal{S}}$ and $P_2^c(\mathbb{R}) \subset \tilde{\mathcal{S}}$. Taking

$$\mathbf{x} = (x_0, x_1, \dots, x_5, x_6) \in \mathbb{R} \times \underbrace{\mathbb{R}^4 \times \dots \times \mathbb{R}^4}_{5 \text{ copies}} \times \mathbb{R} = \mathbb{R}^{22},$$

we define the shooting operator $F_c : \mathbb{R}^{24} \rightarrow \mathbb{R}^{24}$ as

$$F_c(\mathbf{x}, \tau, \alpha) = \begin{pmatrix} \hat{P}_1^c(x_0) - x_1 \\ \psi_1^c(x_1, s) - x_2 \\ T_1(x_2) - x_3 \\ \phi_\alpha(x_3, \tau) - x_4 \\ T_2^{-1}(x_4) - x_5 \\ \psi_2^c(x_5, s) - \tilde{P}_2^c(x_6) \end{pmatrix}. \quad (54)$$

We have the following result.

Lemma 27. *Suppose that for $c \in \mathbb{R}$ we have an $\mathbf{x}(c) \in \mathbb{R}^{22}$ and $\tau(c) \in \mathbb{R}$ for which*

$$F_c(\mathbf{x}(c), \tau(c), 0) = 0,$$

then we have one of the following three cases:

1. *If $x_0(c) \neq 0$ and $x_6(c) \neq 0$, then the orbit through $T_1(\hat{P}_1^c(x_0(c)))$ is periodic.*
2. *If $x_0(c) = 0$ and $x_6(c) \neq 0$, then the orbit through $T_1(\hat{P}_1^c(x_0(c)))$ is an ejection-collision with m_1 .*
3. *If $x_0(c) \neq 0$ and $x_6(c) = 0$, then the orbit through $T_1(\hat{P}_1^c(x_0(c)))$ is an ejection-collision with m_2 .*

Proof. The result follows immediately from the definition of F_c in Equation (54) and from Theorem 19 (or the analogous theorem for m_2). We highlight the fact that due to Equations (52)–(53) we have $E_1^c(\hat{P}_1^c(x_0)) = 0$ and $E_2^c(\hat{P}_2^c(x_6)) = 0$, so the trajectories in the regularized coordinates correspond to the physical trajectories in the physical coordinates of the PCRTBP. ■

We can use the implicit function theorem to compute the derivative of $\mathbf{x}(c)$ with respect to c . Let us write $\mathbf{y}(c) := (\mathbf{x}(c), \tau(c), \alpha(c))$ and suppose $F_c(\mathbf{y}(c)) = 0$. (Note that in fact we must also have that $\alpha(c) = 0$ since α is unfolding.) Then $\frac{d}{dc}\mathbf{x}(c)$ is computed from the first coordinates of the vector $\frac{d}{dc}\mathbf{y}(c)$ and is given by the formula

$$\frac{d}{dc}\mathbf{y}(c) = - \left(\frac{\partial F_c}{\partial \mathbf{y}} \right)^{-1} \frac{\partial F_c}{\partial c}. \quad (55)$$

Theorem 28. *Assume that for $c \in [c_1, c_2]$ the functions $\mathbf{x}(c)$ and $\tau(c)$ solve the implicit equation*

$$F_c(\mathbf{x}(c), \tau(c), 0) = 0.$$

If

$$x_0(c_1) > 0 > x_0(c_2), \quad (56)$$

$$x_6(c) \neq 0 \quad \text{for all } c \in [c_1, c_2], \quad (57)$$

and

$$\frac{d}{dc}x_0(c) < 0 \quad \text{for all } c \in [c_1, c_2], \quad (58)$$

then there exists a unique energy parameter $c^ \in (c_1, c_2)$ for which we have an intersection of the ejection and collision manifolds of m_1 . Moreover, for all remaining $c \in [c_1, c_2] \setminus \{c^*\}$ the orbit of the point $T_1(\hat{P}_1^c(x_0(c)))$ is periodic.*

Proof. The result follows directly from the Bolzano theorem and Lemma 27. ■

Theorem 28 is deliberately formulated so that its hypotheses can be validated via computer assistance. Specifically, rigorous enclosures of Equation (55) are rigorously computed and Equations (56)–(58) are rigorously verified using interval arithmetic.

We finish this section with an example of a similar approach, which can be used for the proofs of double collisions in the case when $m_1 = m_2 = \frac{1}{2}$. That is, we establish the

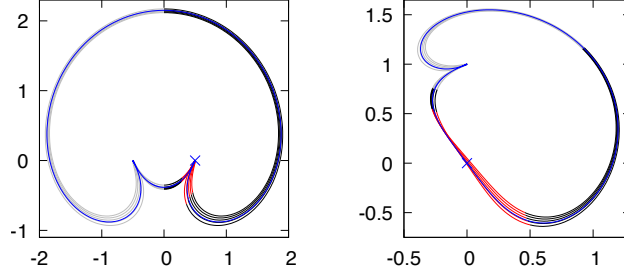


Figure 9: A family of periodic orbits passing through a double collision. The left figure is in the original coordinates and the right figure is in the regularised coordinates at m_1 . The trajectories computed in the original coordinates are in black, the trajectories computed in the regularized coordinates are in red, and the collision orbit is in blue. The second half of an orbit, which follows from the R -symmetry, is depicted in grey. The plots are for the system with equal masses.

existence of a family of periodic orbits, parameterized by energy (the Jacobi constant), which are symmetric with respect to the y -axis, and such that for a single parameter from the family we have a double collision as in Figure 9.

In this case consider $R : \mathbb{R}^4 \rightarrow \mathbb{R}^4$ defined as

$$R(x, p, y, q) = (-x, p, y, -q).$$

For the case of two equal masses, we have the time reversing symmetry

$$R(\phi(\mathbf{x}, t)) = \phi(R(\mathbf{x}), -t). \quad (59)$$

We denote by \mathcal{R} the set of all points which are R -self symmetric, i.e. $\mathcal{R} = \{\mathbf{x} = R(\mathbf{x})\}$. An argument mirroring Equation (51) shows that if two points $\mathbf{x}, \mathbf{y} \in \mathcal{R}$ have $\mathbf{y} = \phi(\mathbf{x}, t)$, then these points must lie on a periodic orbit.

To obtain the existence of the family of orbits depicted in Figure 9, define $p : \mathbb{R}^2 \rightarrow \mathbb{R}$ and $P_1^c, P_2^c : \mathbb{R} \rightarrow \mathbb{R}^4$ as

$$\begin{aligned} p(y, c) &:= \sqrt{2\Omega(0, y) - c}, \\ P_1^c(y) &:= (0, p(y, c), y, 0), \\ P_2^c(y) &:= (0, -p(y, c), y, 0). \end{aligned}$$

Note that $P_1^c(y), P_2^c(y) \in \mathcal{R}$ and $E(P_1^c(y)) = E(P_2^c(y)) = c$ (see Equation (28)). Consider $x_0, x_7 \in \mathbb{R}$ and $x_1, \dots, x_6 \in \mathbb{R}^4$, where

$$x_4 = (s_4, \hat{p}_4, \hat{y}_4, \hat{q}_4) \in \mathbb{R}^4. \quad (60)$$

We emphasize that the first coordinate in x_4 will be used here in a slightly less standard way than in the previous examples. We define also

$$\hat{x}_4 := (0, \hat{p}_4, \hat{y}_4, \hat{q}_4) \in \mathbb{R}^4.$$

We now choose some fixed $s_2, s_5 \in \mathbb{R}$, $s_2, s_5 > 0$, and for

$$\mathbf{x} = (x_0, \dots, x_7) \in \mathbb{R} \times \underbrace{\mathbb{R}^4 \times \dots \times \mathbb{R}^4}_6 \times \mathbb{R} = \mathbb{R}^{26}$$

define the operator $F_c : \mathbb{R}^{26} \times \mathbb{R} \times \mathbb{R} \rightarrow \mathbb{R}^{28}$ as

$$F_c(\mathbf{x}, \tau, \alpha) = \begin{pmatrix} P_1^c(x_0) - x_1 \\ \phi_\alpha(x_1, s_2) - x_2 \\ T_1^{-1}(x_2) - x_3 \\ \psi_1^c(x_3, s_4) - \hat{x}_4 \\ \psi_1^c(\hat{x}_4, s_5) - x_5 \\ T_1(x_5) - x_6 \\ \phi_\alpha(x_6, \tau) - P_2^c(x_7) \end{pmatrix}. \quad (61)$$

Note that in Equation (61) the s_2, s_5 are some fixed parameters, and s_4 is one of the coordinates of \mathbf{x} . We claim that if $F_c(\mathbf{x}, \tau, 0, 0) = 0$ and $\pi_{\hat{y}_4} \mathbf{x} = 0$, then the orbit of x_2 passes through the collision with m_1 . This is because $\hat{x}_4 = (0, \hat{p}_4, \hat{y}_4, \hat{q}_4)$, so that $F_c = 0$ ensures that the point $\psi_1^c(x_3, s_4)$ is zero on the \hat{x}_4 coordinate. So, if $F_c(\mathbf{x}) = 0$ and $\pi_{\hat{y}_4} \mathbf{x} = 0$, then $\pi_{\hat{x}_4, \hat{y}_4} \psi_1^c(x_3, s_4) = 0$ and we arrive at the collision. Moreover, by the R -symmetry of the system in this case we also establish heteroclinic connections between collisions with m_1 and m_2 (see Figure 9).

If on the other hand $F_c = 0$ and $\pi_{\hat{y}_4} \mathbf{x} \neq 0$, then we have a periodic orbit passing near the collisions with m_1 and m_2 . One can prove a result analogous to Theorem 28 with the minor difference being that instead of using x_0 in Equations (56) and (58) we take \hat{y}_4 . We omit the details in order not to repeat the same argument.

7. Computer assisted proofs for collision/near collision orbits

7.1. Newton-Krawczyk method

For a smooth mapping $F : \mathbb{R}^n \rightarrow \mathbb{R}^n$, the following theorem provides sufficient conditions for the existence of a solution of $F(x) = 0$ in the neighborhood of a “good enough” approximate solution. The hypotheses of the theorem require measuring the defect associated with the approximate solution, as well as the quality of a certain condition number for an approximate inverse of the derivative. Theorems of this kind are used widely in computer assisted proofs, and we refer the interested reader to the works of [67, 68, 69, 70, 71, 72, 73, 74] for a more complete overview.

Let $\|\cdot\|$ be a norm in \mathbb{R}^n and let $\overline{B}(x_0, r) \subset \mathbb{R}^n$ denote a closed ball of radius $r \geq 0$ centered at x_0 in that norm.

Theorem 29 (Newton-Krawczyk). *Let $U \subset \mathbb{R}^n$ be an open set and $F : U \rightarrow \mathbb{R}^n$ be at least of class C^2 . Suppose that $x_0 \in U$ and let A be a $n \times n$ matrix. Suppose that $Y, Z, r > 0$ are positive constants such that $\overline{B}(x_0, r) \subset U$ and*

$$\|AF(x_0)\| \leq Y, \quad (62)$$

$$\sup_{x \in \overline{B}(x_0, r)} \|\text{Id} - ADF(x)\| \leq Z. \quad (63)$$

If

$$Zr - r + Y \leq 0, \tag{64}$$

then there is a unique $\hat{x} \in \overline{B}(x_0, r)$ for which $F(\hat{x}) = 0$. Moreover, $DF(\hat{x})$ is invertible.

Proof. The proof is included in [Appendix A](#) for the sake of completeness. ■

The theorem is well suited for applications to computer assisted proofs. To validate the assumptions its enough to compute interval enclosures of the quantities $F(x_0)$ and $DF(B)$, where B is a suitable ball. These enclosures are done using interval arithmetic, and the results are returned as sets (cubes in \mathbb{R}^n and $\mathbb{R}^{n \times n}$) enclosing the correct values. A good choice for the matrix A is any floating point approximate inverse of the derivative of F at x_0 , computed with standard linear algebra packages. The advantage of working with such an approximation is that there is no need to compute a rigorous interval enclosure of a solution of a linear equation (as in the interval Newton method). In higher dimensional problems, solving linear equations can lead to large overestimation (the so called “wrapping effect”).

In our work the evaluation of F and its derivative involves integrating ODEs and variational equations. There are well know general purpose algorithms for solving these problems, and we refer the interested reader to [75, 15, 70]. For parameterizing the invariant manifolds attached to L_4 with interval enclosures, we exploit the techniques discussed in [76] (validated integration is also discussed in this reference).

We remark that our implementations use the IntLab laboratory running under MatLab⁷ and/or the CAPD⁸ C++ library, and recall that the source codes are found at the homepage of MC. See [77] and [13] as references for the usage and the functionality of the libraries.

7.2. Computer assisted existence proofs for ejection-collision orbits

The methodology of Section 4, and especially Lemma 23, is combined with Theorem 29 to obtain the following.

Theorem 1. *Consider the planar PCRTBP with $\mu = 1/4$ and $c = 3.2$. Let*

$$\bar{p} = \begin{pmatrix} -0.564897282072410 \\ 0.978399619177283 \\ -0.099609551141525 \\ -0.751696444982537 \end{pmatrix},$$

$$r = 2.7 \times 10^{-13},$$

and

$$B_r = \{x \in \mathbb{R}^4 : \|x - \bar{p}\| \leq r\},$$

where the norm is the maximum norm on components. Then, there exists a unique $p_* \in B_r$ such that the orbit of p_* is ejected from m_2 (at $x = -1 + \mu, y = 0$), collides

⁷<https://www.tuhh.de/ti3/rump/intlab/>

⁸Computer Assisted Proofs in Dynamics, <http://capd.ii.uj.edu.pl>

$\bar{x}_0 =$	2.945584780500716			
$\bar{x}_1 =$	(0.0,	-1.387134030283961,	0.0,	0.275425456390970)
$\bar{x}_2 =$	(-0.444581369966432,	-1.038375926396089,	0.112026231721142,	0.449167625710802)
$\bar{x}_3 =$	(-0.564897282072410,	0.978399619177283,	-0.099609551141525,	-0.751696444982537)
$\bar{x}_4 =$	(-0.244097430449606,	0.878139982728136,	-0.025435855606099,	0.543608549989376)
$\bar{x}_5 =$	(0.018086991443589,	-0.732714475912918,	-0.703153304556756,	1.254598547822042)
$\bar{x}_6 =$	1.459760691418490			
$\bar{\tau} =$	2.051635871465197			
$\bar{\alpha} =$	0.0			

Table 1: Numerical data used in the proof of Theorem 1, giving the approximate solution of $F = 0$ for the operator (44), whose zeros correspond to the ejection-collision orbits from m_2 to m_1 . We set the mass ratio to $\mu = 1/4$ and Jacobi constant to $c = 3.2$. The resulting orbit is illustrated in Figure 3 (bottom curve).

with m_1 (at $x = \mu, y = 0$), and the total time T from ejection to collision satisfies the estimate

$$2.42710599795 \leq T \leq 2.42710599796.$$

In addition, the ejection manifold of m_2 intersects the collision manifold of m_1 transversely along the orbit of p_* , where transversality is relative to the level set $\{E = 3.2\}$. Moreover, there exists a transverse S -symmetric counterpart ejected from m_1 and colliding with m_2 .

Proof. The first step in the proof is to define an appropriate version of the map F in Equation (44), whose zeros correspond to ejection-collision orbits from m_2 to m_1 . In particular we set $k = 2$ and $l = 1$, and choose (somewhat arbitrarily) the parameter $s = 0.35$ in the definition of the component maps $R_{\tau,\alpha}^1$ and $R_{\tau,\alpha}^5$. The parameter s determines how long to integrate/flow in the regularized coordinates.

Next we compute an approximate zero $\bar{x} \in \mathbb{R}^{24}$ of F using Newton's method. Note that interval arithmetic is not required in this step. The resulting numerical data is recorded in Table 1, and we note that \bar{x}_3 in the table corresponds to \bar{p} in the hypothesis of the theorem. Note also that we take $\bar{\alpha}$ in the approximate solution to be zero.

We define A to be the numerically computed approximate inverse of $DF(\bar{x})$, and let

$$B = \overline{B}(\bar{x}, r_*),$$

denote the closed ball of radius

$$r_* = 2 \times 10^{-12},$$

in the maximum norm about the numerical approximation. (The reader interested in the numerical entries of the Matrix can run the accompanying computer program). We note that the choice of r_* is somewhat arbitrary. (It should be small enough that there is not too much "wrapping", but not so small that there is no $r \leq r_*$ satisfying the hypothesis of Theorem 29).

Using interval arithmetic and validated numerical integration we compute an interval enclosure of the length 24 vector of intervals \mathbf{F} having

$$F(\bar{x}) \in \mathbf{F},$$

and an interval enclosure of a 24×24 interval matrix \mathbf{M} with

$$DF(x) \in \mathbf{M} \quad \text{for all } x \in B.$$

We then check, again using interval arithmetic, that

$$\|\mathbf{AF}\| \in 10^{-12} \times [0.0, 0.26850976470521]$$

and that

$$\|\text{Id} - \mathbf{AM}\| \in 10^{-7} \times [0.0, 0.23119622467860].$$

From these we have

$$\|AF(\bar{x})\| \leq Y < 0.269 \times 10^{-12}$$

and

$$\sup_{x \in B} \|\text{Id} - ADF(x)\| \leq Z < 0.232 \times 10^{-7},$$

though the actual bounds stored in the computer are tighter than those just reported (hence the inequality).

We let

$$r = \sup \left(\frac{Y}{1 - Z} \right) \leq 2.7 \times 10^{-13},$$

and note again that the actual bound stored in the computer is smaller than reported here. We then check, using interval arithmetic, that

$$Zr - r + Y \leq -5.048 \times 10^{-29} < 0.$$

We also note that, since $r \leq r_*$, we have that $\overline{B}(\bar{x}, r) \subset B$, so that

$$\sup_{x \in \overline{B}(\bar{x}, r)} \|\text{Id} - ADF(x)\| \leq Z,$$

on the smaller ball as well.

From this we conclude, via Theorem 29, that there exists a unique $x_* \in \overline{B}(\bar{x}, r) \subset \mathbb{R}^{24}$ so that $F(x_*) = 0$, and moreover that $DF(x_*)$ is invertible. Hence, it now follows from Lemma 23 that there exists a transverse ejection-collision from m_2 to m_1 in the PCRTBP.

Note that the integration time in the standard coordinates

$$\bar{\tau} = 2.051635871465197,$$

is one of the variables of F (we are simply reading this off the table). The rescaled integration time in the regularized coordinates is fixed to be $s = 0.35$. Our programs compute validated bounds on the integrals in Equation (45) and provide interval enclosures for the time each orbit spends in the regularized coordinate systems of m_1 and m_2 respectively. This interval enclosure is

$$T_1 + T_2 \in [0.27116751585137, 0.27116751585615] + [0.10430261063473, 0.10430261063793].$$

Since the true integration time τ_* is in an r -neighborhood of $\bar{\tau}$ it follows that

$$\tau_* \in [2.05163587146492, 2.05163587146547].$$

Interval addition of the three time intervals containing T_1 , T_2 and τ_* provides the desired final bound on the total time of flight given in the theorem.

The connection in the other direction follows from the S -symmetry of the system (see Equation (50)). The computational part of the proof is implemented in IntLab running under MatLab, and took 21 minutes to run on a standard desktop computer. ■

The orbit whose existence is proven in Theorem 1 is illustrated in Figure 3 (lower orbit of the two orbits illustrated in the figure). The higher orbit follows from the S -symmetry of the PCRTBP. We remark that our implementation actually subdivides the time steps $s = 0.35$ in regularized coordinates 50 times, while the time step $\bar{\tau}$ is subdivided 200 times. This only enlarges the size of the system of equations as discussed in Remark 24.

Validation of the $50+200+50 = 300$ steps of Taylor integration, along with the spatial and parametric variational equations, takes most of the computational time for the proof. The choice of the mass $\mu = 1/4$ and the energy $c = 3.2$ was more or less arbitrary and the existence of many similar orbits could be proven using the same method.

7.3. Connections between ejections/collisions and the libration points L_4, L_5

We apply the methodology of Section 5, and especially Lemma 25, in conjunction with Theorem 29 to obtain the following result. The local stable (or unstable) manifolds at L_4 are computed using the methods and implementation of [16]. See Appendix B for a few additional remarks concerning the parameterizations.

Theorem 2. *Consider planar PCRTBP with $\mu = 1/2$ and $c = 3$ is the energy of L_4 . Let*

$$\bar{p} = \begin{pmatrix} 0.003213450375413 \\ 0.197716496638868 \\ -0.404375730348827 \\ 0.696149210661807 \end{pmatrix},$$

$$r = 8.2 \times 10^{-12},$$

and

$$B_r = \{x \in \mathbb{R}^4 : \|x - \bar{p}\| \leq r\}.$$

Then there exists a unique point

$$p_* \in B_r$$

such that the orbit of p_* accumulates to L_4 as $t \rightarrow -\infty$, collides with m_1 (located at $x = \mu, y = 0$) in finite forward time, and the unstable manifold of L_4 intersects the collision set of m_1 transversely along the orbit of p_* , where transversality is relative to level set $\{E = 3\}$.

Proof. The proof is similar to the proof of Theorem 1, and we only sketch the argument. Orbits accumulating to L_4 in backward time and colliding with m_1 are equivalent to zeros of the mapping $F_{i,j}^u$ defined in Equation (48) with $j = 4$ and $i = 1$. We also set the parameter $s = 0.5$, which is the integration time in the regularized coordinates.

The first step is to compute a numerical zero $\bar{x} = (\bar{x}_0, \bar{x}_1, \bar{x}_2, \bar{x}_3, \bar{x}_4, \bar{\tau}, \bar{\alpha}) \in \mathbb{R}^{16}$ of $F_{i,j}^u$. This step exploits Newton's method (no interval arithmetic necessary), and the resulting data is reported in Table 2. Note that $\bar{x}_1 \in \mathbb{R}^4$ from the table is the initial condition \bar{p} in the statement of the theorem. We take A to be a numerically computed

$\bar{x}_0 =$	0.329444389425640			
$\bar{x}_1 =$	(-0.032305434322402,	-0.044152238388004,	0.843244687835647,	0.005057045291404)
$\bar{x}_2 =$	(0.003213450375413,	0.197716496638868,	-0.404375730348827,	0.696149210661807)
$\bar{x}_3 =$	(0.268116630482827,	-0.943915863314079,	-0.754104155383092,	0.671496024758153)
$\bar{x}_4 =$	1.696671399505923			
$\bar{\tau} =$	7.034349085576677			
$\bar{\alpha} =$	0.0			

Table 2: Numerical data providing an approximate zero of the map $F_{i,j}^u$ defined in Equation (48), for $i = 1, j = 4, c = 3, \mu = 1/2$ and $s = 0.5$. The data is used in the proof of Theorem 2, and results in the existence of the L_4 to collision orbit illustrated in the right frame of Figure 5.

approximate inverse of the 16×16 matrix $DF_{i,j}^u(\bar{x})$. Again, the definition of A does not require interval arithmetic.

For the next step we compute interval enclosures of $F(\bar{x})$ and of $DF_{i,j}^u(x)$ for x in a cube of radius $r_* = 5 \times 10^{-9}$ and obtain that

$$\|AF(\bar{x})\| \in 10^{-11} \times [0.0, 0.82147145471154],$$

and that

$$\sup_{x \in B_{r_*}(\bar{x})} \|\text{Id} - ADF_{i,j}^u(x)\| \in [0.0, 0.00151459031904].$$

Using interval arithmetic we compute

$$r = \frac{Y}{1-Z} \leq 8.3 \times 10^{-12},$$

where the actual value stored in the computer is smaller than reported here (and hence the inequality). We then check, using interval arithmetic, that $Zr - r + Y < 0$. Since $r < r_*$, we have that there exists a unique $x_* \in B_r(\bar{x})$ so that $F_{i,j}^u(x_*) = 0$. Moreover, transversality follows from the non-degeneracy of the derivative of $F_{i,j}^u$.

The proof is implemented in IntLab running under MatLab, and took about 30 minutes to run on a standard desktop computer. ■

By replacing the operator $F_{i,j}^u$ with the operator $F_{i,j}^s$ defined in Equation (48), again with $j = 4$ and $i = 1$, we obtain a nonlinear map whose zeros correspond to ejection-to- L_4 orbits. We compute an approximate numerical zero of the resulting operator (the numerical data is given in Table 3) and repeat a nearly identical argument to that above. This results in the existence of a transverse ejection-to- L_4 orbit in the PCRTBP with $\mu = 1/4$ and $c = 3$. The validated error bound for the numerical data has

$$r \leq 1.8 \times 10^{-11},$$

so that the desired orbit passes with in an r -neighborhood of the point

$$\bar{p} = \begin{pmatrix} -0.112449038686947 \\ -0.553321424594493 \\ 0.308527098616200 \\ 0.727049637558896 \end{pmatrix}.$$

In this way we prove the existence of both the orbits illustrated in Figure 5. More precisely, the orbit whose existence is established in Theorem 2 is illustrated in the right frame of the figure, and the orbit discussed in the preceding remarks is illustrated in the left frame.

$\bar{x}_0 =$	1.561515178070094			
$\bar{x}_1 =$	(0.0,	0.018562030958889,	0.0,	1.999913860896684)
$\bar{x}_2 =$	(0.191471460280817,	0.959639244531484,	0.805673853857139,	1.170011720749615)
$\bar{x}_3 =$	(-0.112449038686946,	-0.553321424594493,	0.308527098616200,	0.727049637558895)
$\bar{x}_4 =$	5.229765599216696			
$\bar{\tau} =$	4.673109099822270			
$\bar{\alpha} =$	0.0			

Table 3: Numerical data for an approximate zero of the map $F_{i,j}^s$ defined in Equation (48), with $i = 1$, $j = 4$ and $s = 0.5$. An argument similar to the proof of Theorem 2, using the data in the table, leads to an existence proof for the ejection-to- L_4 orbit illustrated in the left frame of Figure 5.

$\bar{x}_0 =$	1.411845524482813			
$\bar{x}_1 =$	(-0.037058535628028,	-0.007623220519232,	0.873641524369283,	0.033084516464648)
$\bar{x}_2 =$	(-0.243792823114517,	-1.231115802740768,	0.191555403283542,	-0.508371511645513)
$\bar{x}_3 =$	(0.536705934592082,	-1.502936895854406,	0.178454709494811,	-0.106295188690239)
$\bar{x}_4 =$	(-0.504618223339967,	-0.258236025635830,	-0.463683951257916,	-1.155517796520023)
$\bar{x}_5 =$	(-0.460363255327369,	-0.431694933697799,	0.467966743350051,	0.748266448178995)
$\bar{x}_6 =$	5.988827136344083			
$\bar{\tau} =$	4.753189987600258			
$\bar{\alpha} =$	0.0			

Table 4: Numerical data for the proof of Theorem 3, which provides an approximate zero of the L_4 homoclinic map $F_{i,j,k}$ defined in Equation (49), when $i = k = 4$, $j = 2$, $s_1 = 1.8635$, and $s_2 = 5$. The orbit is depicted on the right plot in Figure 6.

7.4. Transverse homoclinics for L_4 and L_5

Combining the methodology of Section 5, and especially Lemma 25, with Theorem 29 we obtain the following result.

Theorem 3. *Consider the planar PCRTBP with $\mu = 1/2$ and $c = 3$ is the energy level of L_4 . Let*

$$\bar{p} = \begin{pmatrix} -0.037058535628028 \\ -0.007623220519232 \\ 0.873641524369283 \\ 0.033084516464648 \end{pmatrix},$$

and

$$B_r = \{x \in \mathbb{R}^4 : \|x - \bar{p}\| \leq r\},$$

where

$$r = 1.6 \times 10^{-9}.$$

Then there exists a unique $p_* \in B_r$ so that the orbit of p_* is homoclinic to L_4 and $W^s(L_4)$ intersects $W^u(L_4)$ transversely along the orbit of p_* , where transversality is relative to the level set $\{E = 3\}$.

Proof. As in the earlier cases, the argument hinges on proving the existence of a zero of a suitable nonlinear mapping, in this case the map $F_{i,j,k}$ defined in Equation (49), with $i = k = 4$ and $j = 2$. The integration time parameters are set as $s_1 = 1.8635$ and $s_2 = 5$. These are the flow times in the regularized coordinates and in the original coordinates (the second time) respectively. With these choices, a zero of $F_{4,2,4}$ corresponds to an orbit homoclinic to L_4 which passes through the Levi-Civita coordinates regularized at m_2 .

The numerical data $\bar{x} \in \mathbb{R}^{24}$ providing an approximate zero of $F_{4,2,4}$ is reported in Table 7.4. Note that x_1 corresponds to \bar{p} in the hypothesis of the theorem. We let A be a numerically computed approximate inverse of the matrix $DF_{4,2,4}(\bar{x})$. The table data and the matrix A are computed using a numerical Newton scheme, and standard double precision floating point operations.

Using validated numerical integration schemes, validated bounds on the local stable/unstable manifold parameterizations, and interval arithmetic, we compute interval enclosures of $F_{4,2,4}(\bar{x})$ and of $DF_{4,2,4}(B_r(\bar{x}))$ with where $r = 1.659487745915747 \times 10^{-9}$. We then check that

$$\|AF(\bar{x})\| \in 10^{-8} \times [0.0, 0.16432156145308],$$

and that

$$\sup_{x \in B_r(\bar{x})} \|\text{Id} - ADF_{4,2,4}(B_r(\bar{x}))\| \in [0.0, 0.00980551463848].$$

Finally, we use interval arithmetic to verify that $Zr - r + Y < 0$ and transversality follows as in the earlier cases which completes the proof. ■

Note that, from a numerical perspective, this is the most difficult computer assisted argument presented so far. This is seen in the fact that $Z \approx 10^{-2}$ and $r \approx 10^{-9}$. That is, these constants are roughly three orders of magnitude less accurate than the previous theorems. On the other hand, the orbit itself is more complicated than those in the previous theorems. We note that the accuracy of the result could be improved by taking smaller integration steps and/or using higher order Taylor approximation. However, this would also increase the required computational time.

Now, by symmetry, the result above gives a transverse homoclinic orbit for L_5 which passes near m_1 . We also observe that each of these transverse homoclinic orbits also satisfy the hypotheses of the theorems of Devaney and Henard discussed in Section 1. In particular, Theorem 3 also proves the existence of a chaotic subsystem in the $c = 3$ energy level of the PCRTBP near the orbit of p_* , and a tube of periodic orbits parameterized by the Jacobi constant which accumulate to the homoclinic orbit through p_* .

We remark that, using similar arguments, we are able to prove also the existence and transversality of the homoclinic orbits in the left and center frames of Figure 6. More precisely, let

$$\bar{p}_1 = \begin{pmatrix} -0.033854025583296 \\ -0.043110876471418 \\ 0.844639632487862 \\ 0.007320747846173 \end{pmatrix}, \quad \bar{p}_2 = \begin{pmatrix} 0.029871559148065 \\ -0.006337684774610 \\ 0.850175365286339 \\ -0.034734413580682 \end{pmatrix},$$

and

$$r_1 = 2.03 \times 10^{-10}, \quad r_2 = 1.84 \times 10^{-8}.$$

Then there exist unique points $p_*^1 \in B(\bar{p}_1, r_1)$ and $p_*^2 \in B(\bar{p}_2, r_2)$ so that $W^{s,u}(L_4)$ intersect transversely along the orbits through these points. It is also interesting to note that r_2 is two orders of magnitude larger than r_1 . This is caused by the fact that the time of flight (integration time) is longer in this case and, more importantly, the fact that the second orbit passes very close to m_1 . Indeed, the error bounds for the second

$\bar{x}_0 =$	0.0			
$\bar{x}_1 =$	(0.0,	2.8111911379251,	0.0,	0.0)
$\bar{x}_2 =$	(0.96886794638213,	-0.3219837525934,	-0.52587590839627,	-2.8644348266831)
$\bar{x}_3 =$	(0.67431017475157,	-0.74811608844773,	-1.0190086228395,	-1.0721803622694)
$\bar{x}_4 =$	(-1.0199016713004,	0.72482377063238,	-0.062207790440189,	1.1639536137604)
$\bar{x}_5 =$	(0.1377088390491,	-0.32616835939217,	-0.22586709346235,	0.6480010784062)
$\bar{x}_6 =$	0.070375791076957			
$\bar{\tau} =$	2.0972398526268			
$\bar{\alpha} =$	0.0			

Table 5: Numerical data for the proof of Theorem 4, which gives an approximate solution to $F_c = 0$ for the operator (54), for which we have a collision of the family of Lyapunov orbits with m_1 for the Earth-Moon system (see Figure 7). This occurs for a unique value of the Jacobi constant $c^* \in \mathbf{c}$.

orbit would very likely be improved by changing to regularized coordinates near m_1 and this may even be necessary to validate some homoclinics passing even closer to m_1 or m_2 . Nevertheless, we were able to validate these orbits in standard coordinates so we have not done this here.

The orbit of p_*^1 is illustrated in the left frame of Figure 6 appears to have y -axis symmetry, however we do not use this symmetry nor do we rigorously prove its existence. The orbit of p_*^2 is illustrated in the center frame of Figure 6 has no apparent symmetry. The orbits illustrated in the left and center frames have appeared previously in the literature, as remarked in Section 1. However, to the best of our knowledge this is the first mathematically rigorous proof of their existence.

7.5. Periodic orbits passing through collision

We apply the methodology of section 6, namely Lemma 27 and Theorem 28, with Theorem 29 to obtain the following result. We consider the Earth-Moon mass ratio largely for the sake of variety.

Theorem 4. *Consider the Earth-Moon system⁹ where m_2 has mass $\mu = 0.0123/1.0123$ and m_1 has mass $1 - \mu$. Let¹⁰*

$$c_0 = 1.4340459493, \quad \text{and} \quad \delta = 10^{-11}.$$

There exists a single value $c^ \in (c_0 - \delta, c_0 + \delta)$ of the Jacobi integral, for which we have an orbit along the intersection of the ejection and collision manifolds of m_1 . Moreover, for every $c \in [c_0 - \delta, c_0 + \delta] \setminus \{c^*\}$ we have an S -symmetric Lyapunov orbit, that passes close to the collision with m_1 . In addition, for every $c \in \{1.2, 1.25, 1.3, \dots, 1.65\}$ there exists a Lyapunov orbit, which passes close the collision with m_1 . (These orbits are depicted in Figure 7.)*

Proof. The orbits for the Jacobi integral values in $\mathbf{c} := [c_0 - \delta, c_0 + \delta]$ were established by means of Theorems 28 and 29. We have first pre-computed numerically (through a standard, non-interval, numerical computation) an approximation $\bar{\mathbf{x}} \in \mathbb{R}^{22}$,

⁹So named because this is the approximate mass ratio of the Moon relative to the Earth.

¹⁰In fact, our numerical calculations suggest that a more accurate value of the Jacobi constant for which we have the collision is 1.434045949300768. However, since in the theorem we obtain only interval results, we round c_0 so that digits smaller than the width of the interval are not used.

$\bar{\tau} \in \mathbb{R}$ for the functions $\mathbf{x}(c)$ and $\tau(c)$, for $c \in \mathbf{c}$. (The $\bar{\mathbf{x}}$ and $\bar{\tau}$ are written out in Table 5.) We then took $\bar{x} := (\bar{\mathbf{x}}, \bar{\tau}, 0) \in \mathbb{R}^{24}$, and a ball $\bar{B}(\bar{x}, r)$, in the maximum norm, with $r = 10^{-11}$. We established using Theorem 29 that $\mathbf{x}(c)$ and $\tau(c)$ satisfying

$$F_c(\mathbf{x}(c), \tau(c), 0) = 0, \quad \text{for } c \in \mathbf{c},$$

are r -close to $\bar{\mathbf{x}}$ and $\bar{\tau}$. To apply Theorem 29 we have used the matrix A to be an approximation of $(DF_c(\bar{\mathbf{x}}, \bar{\tau}, 0))^{-1}$ (computed with standard numerics, without interval arithmetic).

We also checked using interval arithmetic that

$$\begin{aligned} x_0(c_0 - \delta) &\in [3.2261 \cdot 10^{-12}, 5.2262 \cdot 10^{-12}] > 0, \\ x_0(c_0 + \delta) &\in [-4.6229 \cdot 10^{-12}, -2.6228 \cdot 10^{-12}] < 0. \end{aligned}$$

By using Equation (55), we have established the following interval arithmetic bound for the derivative of x_0 with respect to the parameter

$$\frac{d}{dc}x_0(c) \in [-0.53146, -0.25344] < 0 \quad \text{for } c \in \mathbf{c}.$$

We also verified that

$$x_6(c) \in [0.07037579, 0.07037580], \quad \text{for } c \in \mathbf{c},$$

so $x_6(c) \neq 0$. This proves all necessary hypotheses of Theorem 28 are satisfied for the interval \mathbf{c} , which finishes the first part of the proof.

The Lyapunov orbits for $c \in \{1.2, 1.25, 1.3, \dots, 1.65\}$ were established in a similar way. For each value of the Jacobi constant we have non-rigorously computed an approximation of a point for which F_c is close to zero, and validated that we have $F_c = 0$ for a point in a given neighbourhood of each approximation by means of Theorem 28. Then each Lyapunov orbit followed from Lemma 27. The proof was conducted by using the CAPD library [13] and took under 4 seconds on a standard laptop. ■

In a similar way we have used the operator in Equation (61) to prove the following result.

Theorem 5. *Consider the equal masses system where $\mu = \frac{1}{2}$. Let¹¹*

$$c_0 = 2.05991609689, \quad \text{and} \quad \delta = 10^{-11}.$$

There exists a single value $c^ \in (c_0 - \delta, c_0 + \delta)$ of the Jacobi integral, for which we have two intersections of the ejection and collision manifolds of m_1 and m_2 (a double collision). Moreover, for every $c \in [c_0 - \delta, c_0 + \delta] \setminus \{c^*\}$ we have an R -symmetric periodic orbit, that passes close to the collision with both m_1 and m_2 .*

In addition, for every $c \in \{2, 2.05, 2.1, 2.15, 2.2\}$ there exists an R -symmetric periodic orbit, which passes close the collisions with m_1 and m_2 . (See Figure 9.)

¹¹We believe that a more accurate value of the Jacobi constant for which we have the double collision is 2.059916096889689.

$\bar{x}_0 =$	2.1500812504263			
$\bar{x}_1 =$	(0.0,	1.9284591731628,	2.1500812504263,	0.0)
$\bar{y}_1 =$	(0.69048473611567,	1.7931365837031,	2.0235432631366,	-0.68131264815823)
$\bar{y}_2 =$	(1.2840491252838,	1.4060903194974,	1.6633024005717,	-1.2578372410208)
$\bar{y}_3 =$	(1.6975511373876,	0.82331762641153,	1.1255430505039,	-1.635312833307)
$\bar{y}_4 =$	(1.8749336204161,	0.13626785074409,	0.4974554541058,	-1.7408028751654)
$\bar{y}_5 =$	(1.7998279644685,	-0.53073278614628,	-0.11297480280335,	-1.5366473737295)
$\bar{y}_6 =$	(1.5061749347656,	-1.0305902992759,	-0.59342931060715,	-1.0405479042095)
$\bar{y}_7 =$	(1.0818972907729,	-1.2225719420862,	-0.85102013466618,	-0.34180581034401)
$\bar{y}_8 =$	(0.65897461363208,	-1.0129455565064,	-0.83705911740279,	0.41484122714387)
$\bar{x}_2 =$	(0.39363679634804,	-0.35214129843918,	-0.55459777216455,	1.118144276789)
$\bar{x}_3 =$	(0.47871801188109,	-1.6325298121847,	-0.5792530867862,	0.66259374214967)
$\bar{x}_4 =$	(0.40239981358785 ,	-1.0164469492932,	0.0,	1.7224504635177)
$\bar{x}_5 =$	(-0.25865224139372,	-0.43561054122851,	0.51876042853484,	1.7861707478994)
$\bar{x}_6 =$	(0.29778859976434,	-1.2111468567795,	-0.2683570951738,	-1.0237309759288)
$\bar{x}_7 =$	-0.38367247647373			
$\bar{\tau} =$	0.24444305938687			
$\bar{\alpha} =$	0.0			

Table 6: Numerical data for the proof of Theorem 5 giving an approximate solution to $F_c = 0$, for the operator (61), for $c = 2.05991609689$ for which we have a double collision of a family of R -symmetric periodic orbits for the equal masses system; see Figure 9. In the bold font we have singled out the first coefficient of x_4 , which is the time s_4 and not the physical coordinate of the collision point, for which we have $\hat{x} = 0$. (See Equations (60) and (61).)

Proof. The proof follows along the same lines as the proof of Theorem 4. We do not write out the details of all the estimates since we feel that this brings little added value¹². In the operator F_c from Equation (61) we have taken $s_2 = 3.3$ and $s_5 = 0.3$. The fact that s_2 involves a long integration time caused a technical problem for us in obtaining an estimate for $\frac{d}{dc}\pi_{\hat{y}}\mathbf{x}(c)$. To get a good enough estimate to establish that $\frac{d}{dc}\pi_{\hat{y}}\mathbf{x}(c) > 0$ we needed to include additional points y_1, \dots, y_m in the shooting scheme and extend F_c to include

$$\phi_\alpha(x_1, s) - y_1, \quad \phi_\alpha(y_1, s) - y_2, \quad \dots \quad \phi_\alpha(y_{m-1}, s) - y_m, \quad \phi_\alpha(y_m, s) - x_2,$$

where $s = s_2/(m+1)$. We took $m = 8$, and the point X_0 which serves as our approximation for $F_c = 0$ is written out in Table 6. The proof took under 10 seconds on a standard laptop. ■

Remark 30 (MatLab with IntLab versus CAPD). We note that the computer programs implemented in C^{++} using the CAPD library run much faster than the programs implemented in MatLab using IntLab to manage the interval arithmetic. This is not surprising, as compiled programs typically run several hundred times faster than MatLab programs, and the use of interval arithmetic only complicates things. Moreover, CAPD is a well tested, optimized, general purpose package, while our IntLab codes were written specifically for this project. The CAPD library, due to its efficient integrators, allowed us to perform almost all of the proofs without subdividing the time steps, which was needed for the MatLab code (see Remark 24 and comments at the end of section 7.2), except for the proof of Theorem 5 (see Table 6). In particular, little time has been spent on optimizing these codes. Nevertheless, it is nice to have rigorous integrators implemented in multiple languages, and the codes for validating the 2D stable/unstable manifolds at L_4 were written in IntLab and have not been ported to C^{++} .

¹²The code for the proof is made available on the personal web page of Maciej Capiński.

Appendix A.

Proof of Theorem 29. From Equation (64) and since $r > 0$ we see that $Z + \frac{Y}{r} \leq 1$, which since $Y, r > 0$ gives

$$Z < 1. \quad (\text{A.1})$$

Now, define the Newton operator

$$T(x) = x - AF(x). \quad (\text{A.2})$$

For $x_1, x_2 \in \overline{B}(x_0, r)$, by the mean value theorem and (63), we see that

$$\begin{aligned} \|T(x_1) - T(x_2)\| &\leq \sup_{x \in \overline{B}(x_0, r)} \|DT(x)\| \|x_1 - x_2\| \\ &= \sup_{x \in \overline{B}(x_0, r)} \|\text{Id} - ADF(x)\| \|x_1 - x_2\| \\ &\leq Z \|x_1 - x_2\|, \end{aligned}$$

and since $Z < 1$ we conclude that T is a contraction on $\overline{B}(x_0, r)$.

To see that T maps $\overline{B}(x_0, r)$ into itself, for $x \in \overline{B}(x_0, r)$ by Equations (62)–(64) we have

$$\begin{aligned} \|T(x) - x_0\| &\leq \|T(x) - T(x_0)\| + \|T(x_0) - x_0\| \\ &\leq \sup_{x \in \overline{B}(x_0, r)} \|DT(z)\| \|x - x_0\| + \|AF(x_0)\| \\ &\leq Zr + Y \\ &\leq r \end{aligned}$$

hence $T(x) \in \overline{B}(x_0, r)$.

By the Banach contraction mapping theorem there is a unique $\hat{x} \in \overline{B}(x_0, r)$ so that

$$T(\hat{x}) = \hat{x}. \quad (\text{A.3})$$

Now observe that for every $x \in \overline{B}(x_0, r)$, including \hat{x} , by Equations (63) and (A.1) we have that

$$\|\text{Id} - ADF(\hat{x})\| \leq Z < 1.$$

Then

$$ADF(\hat{x}) = \text{Id} - (\text{Id} - ADF(\hat{x})) = \text{Id} - B$$

with $\|B\| < 1$. By the Neumann series theorem we see that $ADF(\hat{x})$ is invertible. It therefore follows that both A and $DF(\hat{x})$ are also invertible.

From Equations (A.2) and (A.3) we see that $AF(\hat{x}) = 0$. But A is invertible, so it follows that $F(\hat{x}) = 0$, as required. ■

Appendix B.

Here follows a terse description of the local stable/unstable manifold parameterizations used in the proofs in Sections 7.3 and 7.4. Much more complete information is found in [16, 78, 79]. In the present discussion $f: U \rightarrow \mathbb{R}^d$ denotes the (real analytic) PCRTB vector field, and L_j is one of the equilateral triangle libration points – so that $j = 4, 5$. We are interested in parameter values where $Df(L_{4,5})$ has complex conjugate stable/unstable eigenvalues

$$\pm\alpha \pm i\beta,$$

with $\alpha, \beta > 0$. We write $\lambda = -\alpha + i\beta$ when considering the stable manifold, and $\lambda = \alpha + i\beta$ when considering the unstable.

Our goal is to develop a formal series expansion of the form

$$w_j^\kappa(z_1, z_2) = \sum_{m=0}^{\infty} \sum_{n=0}^{\infty} p_{mn} z_1^m z_2^n, \quad (\text{B.1})$$

where $j = 4$ or 5 depending on whether we are based at L_4 or L_5 , and $\kappa = s$ or u depending on whether we are considering the stable or unstable manifold. Here $p_{mn} \in \mathbb{C}^4$ for all $(m, n) \in \mathbb{N}^2$. Moreover, we take

$$p_{00} = L_j,$$

where $j = 4, 5$, and

$$p_{10} = \xi, \quad \text{and} \quad p_{01} = \bar{\xi},$$

where $\xi, \bar{\xi} \in \mathbb{C}^4$ are complex conjugate eigenvectors associated with the complex conjugate eigenvalues $\lambda, \bar{\lambda} \in \mathbb{C}$.

We use the parameterization method to characterize w_j^κ . While we refer the interested reader to [78, 79] for much more complete discussion of this method, we remark that the main idea is to solve the invariance equation

$$\lambda z_1 \frac{\partial}{\partial z_1} w_j^\kappa(z_1, z_2) + \bar{\lambda} z_2 \frac{\partial}{\partial z_2} w_j^\kappa(z_1, z_2) = f(w_j^\kappa(z_1, z_2)), \quad (\text{B.2})$$

subject to the constraints

$$w_j^\kappa(0, 0) = L_j, \quad \frac{\partial}{\partial v} w_j^\kappa(0, 0) = \xi, \quad \text{and} \quad \frac{\partial}{\partial w} w_j^\kappa(0, 0) = \bar{\xi}.$$

It can be shown that if w_j^κ solves Equation (B.2) subject to these constraints, then it parameterizes a local stable/unstable manifold at L_j .

To solve Equation (B.2) numerically we insert the power series ansatz of Equation (B.1), expand the nonlinearities, and match like powers of z_1 and z_2 . This procedure leads to homological equations of the form

$$(Df(p_{00}) - (m\lambda + n\bar{\lambda})\text{Id}) p_{mn} = \mathcal{R}_{mn},$$

describing the power series coefficients p_{mn} for $m + n \geq 2$. Here \mathcal{R}_{mn} is a nonlinear function of the coefficients of order less than $m + n$, whose computation in the case of

$m \setminus n$	0	1	2
0	$\begin{pmatrix} 0.0 \\ 0.0 \\ 0.866 \\ 0.0 \end{pmatrix}$	$\begin{pmatrix} 0.012 + 0.018i \\ -0.025 \\ -0.015 + 0.0067i \\ 0.0034 - 0.019i \end{pmatrix}$	$10^{-3} \begin{pmatrix} -0.050 + 0.076i \\ -0.081 - 0.190i \\ -0.054 - 0.041i \\ 0.140 - 0.051i \end{pmatrix}$
1	$\begin{pmatrix} 0.012 - 0.018i \\ -0.025 \\ -0.015 - 0.0067i \\ 0.0034 + 0.019i \end{pmatrix}$	$10^{-3} \begin{pmatrix} 0.37 \\ -0.47 \\ -0.09 \\ 0.12 \end{pmatrix}$	$10^{-4} \begin{pmatrix} 0.041 + 0.055i \\ -0.130 - 0.070i \\ -0.036 - 0.048i \\ 0.110 + 0.060i \end{pmatrix}$
2	$10^{-3} \begin{pmatrix} -0.050 - 0.076i \\ -0.081 + 0.190i \\ -0.054 + 0.041i \\ 0.140 + 0.051i \end{pmatrix}$	$10^{-4} \begin{pmatrix} 0.041 - 0.055i \\ -0.130 + 0.070i \\ -0.036 + 0.048i \\ 0.110 - 0.060i \end{pmatrix}$	0

$$p_{03} = 10^{-5} \begin{pmatrix} -0.14 + 0.18i \\ -0.26 - 0.76i \\ 0.11 + 0.09i \\ -0.47 + 0.11i \end{pmatrix} \quad p_{30} = 10^{-5} \begin{pmatrix} -0.14 - 0.18i \\ -0.26 + 0.76i \\ 0.11 - 0.09i \\ -0.47 - 0.11i \end{pmatrix}$$

Table B.7: Approximate power series coefficients p_{mn} for the parameterization of the local stable manifold of L_4 for the equal masses case $\mu = 1/2$.

the PCRTBP is discussed in more detail in [16]. Note that if f is real analytic, then the coefficients have the symmetry

$$p_{nm} = \overline{p_{mn}},$$

and we obtain the real image of \mathcal{P} by evaluating on complex conjugate variables $w = \bar{v}$.

Since the order zero and order 1 coefficients are determined by L_j and its eigendata, we can compute p_{mn} for all $2 \leq m+n \leq N$ by recursively solving the linear homological equations to any desired order $N \geq 2$. We obtain the approximation

$$w_j^{\kappa, N}(z_1, z_2) = \sum_{m+n=0}^N p_{mn} z_1^m z_2^n.$$

For example, in the PCRTBP with $\mu = 1/2$, Table B.7 shows approximate coefficients for the stable manifold at L_4 , computed to order $N = 3$. The data has been truncated at only two or three significant figures to make it fit in the table. Note that the complex conjugate structure of the coefficients is seen in the table. The table is included to give the reader a sense of the form of the data in these calculations, and could be used to very approximately reproduce some of the results in the present work.

For the calculations in the main body of the text, we take $N = 12$ and compute the p_{mn} by recursively solving the homological equations using interval arithmetic. Moreover, using the a-posteriori analysis developed in [17], we obtain a bound of the form

$$\sum_{m+n=13}^{\infty} \|p_{mn}\| \leq 1.4 \times 10^{-13},$$

on the norm of the tail of the parameterization. The analysis is very similar to the a-posteriori analysis of the Newton Krawczyk Theorem 29 promoted in the present work, adapted to the context of Banach spaces of infinite sequences.

Note that this “little ell one” norm bounds the C^0 norm of the truncation error on the unit disk, and that Cauchy bounds can be used to estimate derivatives of the

parameterization on any smaller disk. Thus we actually take

$$P_j^\kappa(\theta) = w_j^\kappa(0.9 \cos(\theta) + 0.9 \sin(\theta)i, 0.9 \cos(\theta) - 0.9 \sin(\theta)i),$$

as our local parameterization, where

$$w_j^\kappa(z_1, z_2) = w_j^{\kappa, N}(z_1, z_2) + w_j^{\kappa, \infty}(z_1, z_2),$$

is a polynomial plus a tail which has

$$w_j^{\kappa, \infty}(z_1, z_2) = \sum_{n+m=N+1}^{\infty} p_{mn} z_1^m z_2^n,$$

and

$$\sup_{|z_1|, |z_2| < 1} \|w_j^{\kappa, \infty}(z_1, z_2)\| \leq 1.4 \times 10^{-13}.$$

The 0.9 gives up a portion of the disk, allowing us to bound the derivatives needed in the Newton-Kantorovich argument.

References

- [1] J. Henrard, [Proof of a conjecture of E. Strömberg](#), *Celestial Mech.* 7 (1973) 449–457. URL <https://doi-org.ezproxy.fau.edu/10.1007/BF01227510>
- [2] R. L. Devaney, Homoclinic orbits in Hamiltonian systems, *J. Differential Equations* 21 (2) (1976) 431–438.
- [3] V. Szebehely, *Theory of Orbits*, Academic Press Inc., 1967.
- [4] A. J. Maciejewski, S. M. Rybicki, [Global bifurcations of periodic solutions of the Hill lunar problem](#), *Celestial Mech. Dynam. Astronom.* 81 (4) (2001) 279–297. doi:10.1023/A:1013276830424. URL <https://doi.org/10.1023/A:1013276830424>
- [5] A. J. Maciejewski, S. M. Rybicki, [Global bifurcations of periodic solutions of the restricted three body problem](#), *Celestial Mech. Dynam. Astronom.* 88 (3) (2004) 293–324. doi:10.1023/B:CELE.0000017193.10060.ac. URL <https://doi.org/10.1023/B:CELE.0000017193.10060.ac>
- [6] E. Pérez-Chavela, S. a. Rybicki, [Topological bifurcations of central configurations in the \$N\$ -body problem](#), *Nonlinear Anal. Real World Appl.* 14 (1) (2013) 690–698. doi:10.1016/j.nonrwa.2012.07.027. URL <https://doi.org/10.1016/j.nonrwa.2012.07.027>
- [7] C. García-Azpeitia, J. Ize, [Global bifurcation of planar and spatial periodic solutions from the polygonal relative equilibria for the \$n\$ -body problem](#), *J. Differential Equations* 254 (5) (2013) 2033–2075. doi:10.1016/j.jde.2012.08.022. URL <https://doi.org/10.1016/j.jde.2012.08.022>
- [8] C. García-Azpeitia, J. Ize, [Global bifurcation of planar and spatial periodic solutions in the restricted \$n\$ -body problem](#), *Celestial Mech. Dynam. Astronom.* 110 (3) (2011) 217–237. doi:10.1007/s10569-011-9354-2. URL <https://doi.org/10.1007/s10569-011-9354-2>
- [9] U. S. R. Association. [Earth’s oldest rock found on the moon](#) [online] (January 2019).
- [10] F. Moulton, D. Buchanan, T. Buck, F. Griffin, W. Longley, W. MacMillan, *Periodic Orbits*, no. Publication No. 161, Carnegie Institution of Washington, 1920.
- [11] V. Szebehely, On Moulton’s orbits in the restricted problem of three bodies, *Proceedings of the National Academy of (S)cience of the United States of America* 56 (6) (1966) pp. 1641–1645.
- [12] V. Szebehely, F. T.V., A family of retrograde orbits around the triangular equilibrium points, *The Astronomical Journal* 72 (3) (1967) 373–379.
- [13] T. Kapela, M. Mrozek, D. Wilczak, P. Zgliczyński, [CAPD::DynSys: A flexible c++ toolbox for rigorous numerical analysis of dynamical systems](#), *Communications in Nonlinear Science and Numerical Simulation* 101 (2021) 105578. doi:https://doi.org/10.1016/j.cnsns.2020.105578. URL <https://www.sciencedirect.com/science/article/pii/S1007570420304081>

- [14] P. Zgliczynski, C^1 Lohner algorithm, *Found. Comput. Math.* 2 (4) (2002) 429–465. doi:10.1007/s102080010025.
- [15] D. Wilczak, P. Zgliczynski, c^n -lohner algorithm, *Scheade Informaticae* 20 (2011) 9–46.
- [16] S. Kepley, J. D. Mireles James, **Chaotic motions in the restricted four body problem via Devaney’s saddle-focus homoclinic tangle theorem**, *J. Differential Equations* 266 (4) (2019) 1709–1755. doi:10.1016/j.jde.2018.08.007.
URL <https://doi-org.ezproxy.fau.edu/10.1016/j.jde.2018.08.007>
- [17] J. D. Mireles James, Validated numerics for equilibria of analytic vector fields: invariant manifolds and connecting orbits, in: *Rigorous numerics in dynamics*, Vol. 74 of *Proc. Sympos. Appl. Math.*, Amer. Math. Soc., Providence, RI, 2018, pp. 27–80.
- [18] T. Levi-Civita, **Sur la régularisation du problème des trois corps**, *Acta Math.* 42 (1) (1920) 99–144. doi:10.1007/BF02404404.
URL <https://doi.org/10.1007/BF02404404>
- [19] A. Celletti, Basics of regularization theory, in: B. Stevens, A. Maciejewski, H. M. (Eds.), *Chaotic Worlds: From Order to Disorder in Gravitational N-Body Dynamical Systems*, Springer, Dordrecht, 2006.
- [20] R. L. Devaney, Singularities in classical mechanical systems, in: *Ergodic theory and dynamical systems, I* (College Park, Md., 1979–80), Vol. 10 of *Progr. Math.*, Birkhäuser, Boston, Mass., 1981, pp. 211–333.
- [21] R. McGehee, Singularities in classical celestial mechanics, in: *Proceedings of the International Congress of Mathematicians (Helsinki, 1978)*, Acad. Sci. Fennica, Helsinki, 1980, pp. 827–834.
- [22] R. McGehee, **Triple collision in the collinear three-body problem**, *Invent. Math.* 27 (1974) 191–227. doi:10.1007/BF01390175.
URL <https://doi.org/10.1007/BF01390175>
- [23] R. Moeckel, R. Montgomery, **Symmetric regularization, reduction and blow-up of the planar three-body problem**, *Pacific J. Math.* 262 (1) (2013) 129–189. doi:10.2140/pjm.2013.262.129.
URL <https://doi.org/10.2140/pjm.2013.262.129>
- [24] D. G. Saari, **Improbability of collisions in Newtonian gravitational systems**, *Trans. Amer. Math. Soc.* 162 (1971) 267–271; erratum, *ibid.* 168 (1972), 521. doi:10.2307/1995752.
URL <https://doi.org/10.2307/1995752>
- [25] D. G. Saari, **Improbability of collisions in Newtonian gravitational systems. II**, *Trans. Amer. Math. Soc.* 181 (1973) 351–368. doi:10.2307/1996638.
URL <https://doi.org/10.2307/1996638>
- [26] M. Guardia, V. Kaloshin, J. Zhang, **Asymptotic density of collision orbits in the restricted circular planar 3 body problem**, *Arch. Ration. Mech. Anal.* 233 (2) (2019) 799–836. doi:10.1007/s00205-019-01368-7.
URL <https://doi.org/10.1007/s00205-019-01368-7>
- [27] C. Simó, Analysis of triple collision in the isosceles problem, in: *Classical mechanics and dynamical systems* (Medford, Mass., 1979), Vol. 70 of *Lecture Notes in Pure and Appl. Math.*, Dekker, New York, 1981, pp. 203–224.
- [28] E. A. Belbruno, **A new regularization of the restricted three-body problem and an application**, *Celestial Mech.* 25 (4) (1981) 397–415. doi:10.1007/BF01234179.
URL <https://doi.org/10.1007/BF01234179>
- [29] J. Llibre, **On the restricted three-body problem when the mass parameter is small**, *Celestial Mech.* 28 (1-2) (1982) 83–105. doi:10.1007/BF01230662.
URL <https://doi.org/10.1007/BF01230662>
- [30] J. Delgado Fernández, **Transversal ejection-collision orbits in Hill’s problem for $C \gg 1$** , *Celestial Mech.* 44 (3) (1988/89) 299–307. doi:10.1007/BF01235542.
URL <https://doi.org/10.1007/BF01235542>
- [31] C. Pinyol, **Ejection-collision orbits with the more massive primary in the planar elliptic restricted three body problem**, *Celestial Mech. Dynam. Astronom.* 61 (4) (1995) 315–331.
URL <https://doi-org.ezproxy.fau.edu/10.1007/BF00049513>
- [32] A. Chenciner, J. Llibre, **A note on the existence of invariant punctured tori in the planar circular restricted three-body problem**, *Ergodic Theory Dynam. Systems* 8* (Charles Conley Memorial Issue) (1988) 63–72. doi:10.1017/S0143385700009330.
URL <https://doi.org/10.1017/S0143385700009330>
- [33] J. Féjóz, **Averaging the planar three-body problem in the neighborhood of double inner collisions**, *J. Differential Equations* 175 (1) (2001) 175–187. doi:10.1006/jdeq.2000.3972.
URL <https://doi.org/10.1006/jdeq.2000.3972>

- [34] J. Féjoz, *Quasiperiodic motions in the planar three-body problem*, J. Differential Equations 183 (2) (2002) 303–341. doi:10.1006/jdeq.2001.4117.
URL <https://doi.org/10.1006/jdeq.2001.4117>
- [35] L. Zhao, *Quasi-periodic almost-collision orbits in the spatial three-body problem*, Comm. Pure Appl. Math. 68 (12) (2015) 2144–2176. doi:10.1002/cpa.21539.
URL <https://doi.org/10.1002/cpa.21539>
- [36] S. V. Bolotin, R. S. Mackay, *Periodic and chaotic trajectories of the second species for the n -centre problem*, Celestial Mech. Dynam. Astronom. 77 (1) (2000) 49–75 (2001). doi:10.1023/A:1008393706818.
URL <https://doi.org/10.1023/A:1008393706818>
- [37] S. Bolotin, R. S. MacKay, *Nonplanar second species periodic and chaotic trajectories for the circular restricted three-body problem*, Celestial Mech. Dynam. Astronom. 94 (4) (2006) 433–449. doi:10.1007/s10569-006-9006-0.
URL <https://doi.org/10.1007/s10569-006-9006-0>
- [38] S. Bolotin, *Shadowing chains of collision orbits for the elliptic 3-body problem*, in: SPT 2004—Symmetry and perturbation theory, World Sci. Publ., Hackensack, NJ, 2005, pp. 51–58. doi:10.1142/9789812702142_0007.
URL https://doi.org/10.1142/9789812702142_0007
- [39] S. Bolotin, *Symbolic dynamics of almost collision orbits and skew products of symplectic maps*, Nonlinearity 19 (9) (2006) 2041–2063. doi:10.1088/0951-7715/19/9/003.
URL <https://doi.org/10.1088/0951-7715/19/9/003>
- [40] S. Bolotin, *Shadowing chains of collision orbits*, Discrete Contin. Dyn. Syst. 14 (2) (2006) 235–260. doi:10.3934/dcds.2006.14.235.
URL <https://doi.org/10.3934/dcds.2006.14.235>
- [41] M. Ollé, O. Rodríguez, J. Soler, *Ejection-collision orbits in the RTBP*, Commun. Nonlinear Sci. Numer. Simul. 55 (2018) 298–315. doi:10.1016/j.cnsns.2017.07.013.
URL <https://doi.org/10.1016/j.cnsns.2017.07.013>
- [42] M. Alvarez-Ramírez, E. Barrabés, M. Medina, M. Ollé, *Ejection-collision orbits in the symmetric collinear four-body problem*, Commun. Nonlinear Sci. Numer. Simul. 71 (2019) 82–100. doi:10.1016/j.cnsns.2018.10.026.
URL <https://doi.org/10.1016/j.cnsns.2018.10.026>
- [43] M. Ollé, O. Rodríguez, J. Soler, *Analytical and numerical results on families of n -ejection-collision orbits in the RTBP*, Commun. Nonlinear Sci. Numer. Simul. 90 (2020) 105294, 27. doi:10.1016/j.cnsns.2020.105294.
URL <https://doi.org/10.1016/j.cnsns.2020.105294>
- [44] M. Ollé, O. Rodríguez, J. Soler, *Transit regions and ejection/collision orbits in the RTBP*, Commun. Nonlinear Sci. Numer. Simul. 94 (2021) 105550, 29. doi:10.1016/j.cnsns.2020.105550.
URL <https://doi.org/10.1016/j.cnsns.2020.105550>
- [45] M. Alvarez-Ramírez, E. Barrabés, M. Medina, M. Ollé, *Ejection-collision orbits in two degrees of freedom problems in celestial mechanics*, J. Nonlinear Sci. 31 (4) (2021) Paper No. 68, 33. doi:10.1007/s00332-021-09721-5.
URL <https://doi.org/10.1007/s00332-021-09721-5>
- [46] T. M. Seara, M. Ollé, O. Rodríguez, J. Soler, *Generalised analytical results on n -ejection-collision orbits in the rtbp: analysis of bifurcations*, (Submitted) (2022).
- [47] E. E. Zotos, *Investigating the planar circular restricted three-body problem with strong gravitational field*, Meccanica 52 (9) (2017) 1995–2021. doi:10.1007/s11012-016-0548-2.
URL <https://doi.org/10.1007/s11012-016-0548-2>
- [48] B. Kumar, R. L. Anderson, R. de la Llave, *Rapid and accurate methods for computing whiskered tori and their manifolds in periodically perturbed planar circular restricted 3-body problems*, Celestial Mech. Dynam. Astronom. 134 (1) (2022) Paper No. 3, 38. doi:10.1007/s10569-021-10057-1.
URL <https://doi.org/10.1007/s10569-021-10057-1>
- [49] G. Arioli, *Branches of periodic orbits for the planar restricted 3-body problem*, Discrete Contin. Dyn. Syst. 11 (4) (2004) 745–755. doi:10.3934/dcds.2004.11.745.
URL <http://dx.doi.org.ezproxy.fau.edu/10.3934/dcds.2004.11.745>
- [50] G. Arioli, V. Barutello, S. Terracini, *A new branch of Mountain Pass solutions for the choreographical 3-body problem*, Comm. Math. Phys. 268 (2) (2006) 439–463. doi:10.1007/s00220-006-0111-4.
URL <http://dx.doi.org.ezproxy.fau.edu/10.1007/s00220-006-0111-4>
- [51] T. Kapela, C. Simó, *Computer assisted proofs for nonsymmetric planar choreographies and for stability of the Eight*, Nonlinearity 20 (5) (2007) 1241–1255. doi:10.1088/0951-7715/20/5/010.

- [52] R. C. Calleja, E. J. Doedel, C. García-Azpeitia, *Choreographies in the n -vortex problem*, Regul. Chaotic Dyn. 23 (5) (2018) 595–612. doi:10.1134/S156035471805009X.
URL <https://doi-org.ezproxy.fau.edu/10.1134/S156035471805009X>
- [53] I. Walawska, D. Wilczak, *Validated numerics for period-tupling and touch-and-go bifurcations of symmetric periodic orbits in reversible systems*, Commun. Nonlinear Sci. Numer. Simul. 74 (2019) 30–54. doi:10.1016/j.cnsns.2019.03.005.
URL <https://doi.org/10.1016/j.cnsns.2019.03.005>
- [54] G. Arioli, *Periodic orbits, symbolic dynamics and topological entropy for the restricted 3-body problem*, Comm. Math. Phys. 231 (1) (2002) 1–24. doi:10.1007/s00220-002-0666-7.
URL <http://dx.doi.org.ezproxy.fau.edu/10.1007/s00220-002-0666-7>
- [55] D. Wilczak, P. Zgliczynski, *Heteroclinic connections between periodic orbits in planar restricted circular three-body problem—a computer assisted proof*, Comm. Math. Phys. 234 (1) (2003) 37–75. doi:10.1007/s00220-002-0709-0.
URL <http://dx.doi.org.proxy.libraries.rutgers.edu/10.1007/s00220-002-0709-0>
- [56] M. J. Capiński, *Computer assisted existence proofs of Lyapunov orbits at L_2 and transversal intersections of invariant manifolds in the Jupiter-Sun PCR3BP*, SIAM J. Appl. Dyn. Syst. 11 (4) (2012) 1723–1753. doi:10.1137/110847366.
URL <http://dx.doi.org/10.1137/110847366>
- [57] J. Galante, V. Kaloshin, *Destruction of invariant curves in the restricted circular planar three-body problem by using comparison of action*, Duke Math. J. 159 (2) (2011) 275–327. doi:10.1215/00127094-1415878.
URL <https://doi.org/10.1215/00127094-1415878>
- [58] M. Capiński, M. Guardia, P. Martín, T. M. Seara, P. Zgliczyński, *Oscillatroy motions and parabolic manifolds at infinity in the planar circular restricted three body problem*, Journal of Differential Equations 320 (3) (2022) 316–370.
- [59] M. Capiński, P. Roldán, *Existence of a center manifold in a practical domain around L_1 in the restricted three body problem*, SIAM J. Appl. Dyn. Syst. 11 (1) (2011) 285–318.
- [60] M. Capiński, N. Wodka, *Computer assisted proof of drift orbits along normally hyperbolic manifolds ii: applications to the restricted three body problem*, (Submitted) (2021).
- [61] M. Capiński, M. Gidea, *Arnold diffusion, quantitative estimates and stochastic behavior in the three-body problem*, Communications on Pure and Applied Mathematics (2018).
- [62] A. Celletti, L. Chierchia, *A computer-assisted approach to small-divisors problems arising in Hamiltonian mechanics*, in: Computer aided proofs in analysis (Cincinnati, OH, 1989), Vol. 28 of IMA Vol. Math. Appl., Springer, New York, 1991, pp. 43–51.
URL https://doi-org.ezproxy.fau.edu/10.1007/978-1-4613-9092-3_6
- [63] R. de la Llave, D. Rana, *Accurate strategies for K.A.M. bounds and their implementation*, in: Computer aided proofs in analysis (Cincinnati, OH, 1989), Vol. 28 of IMA Vol. Math. Appl., Springer, New York, 1991, pp. 127–146. doi:10.1007/978-1-4613-9092-3_12.
URL http://dx.doi.org/10.1007/978-1-4613-9092-3_12
- [64] J.-L. Figueras, A. Haro, A. Luque, *Rigorous computer assisted application of kam theory: a modern approach*, (Submitted) arXiv:1601.00084 [math.DS] (2016).
- [65] F. Gabern, A. Jorba, U. Locatelli, *On the construction of the Kolmogorov normal form for the Trojan asteroids*, Nonlinearity 18 (4) (2005) 1705–1734. doi:10.1088/0951-7715/18/4/017.
URL <https://doi.org/10.1088/0951-7715/18/4/017>
- [66] C. Caracciolo, U. Locatelli, *Computer-assisted estimates for Birkhoff normal forms*, J. Comput. Dyn. 7 (2) (2020) 425–460. doi:10.3934/jcd.2020017.
URL <https://doi.org/10.3934/jcd.2020017>
- [67] R. E. Moore, Interval analysis, Prentice-Hall Inc., Englewood Cliffs, N.J., 1966.
- [68] A. Neumaier, Interval methods for systems of equations, Vol. 37 of Encyclopedia of Mathematics and its Applications, Cambridge University Press, Cambridge, 1990.
- [69] A. Neumaier, S. Zu He, *The Krawczyk operator and Kantorovich’s theorem*, J. Math. Anal. Appl. 149 (2) (1990) 437–443. doi:10.1016/0022-247X(90)90053-I.
URL [https://doi.org/10.1016/0022-247X\(90\)90053-I](https://doi.org/10.1016/0022-247X(90)90053-I)
- [70] W. Tucker, Validated numerics, Princeton University Press, Princeton, NJ, 2011, a short introduction to rigorous computations.
- [71] S. M. Rump, *Verification methods: rigorous results using floating-point arithmetic*, Acta Numer. 19 (2010) 287–449. doi:10.1017/S096249291000005X.
URL <http://dx.doi.org/10.1017/S096249291000005X>
- [72] M. T. Nakao, M. Plum, Y. Watanabe, *Numerical verification methods and computer-assisted proofs*

- for partial differential equations, Vol. 53 of Springer Series in Computational Mathematics, Springer, Singapore, [2019] ©2019. doi:10.1007/978-981-13-7669-6.
 URL <https://doi.org/10.1007/978-981-13-7669-6>
- [73] J. B. van den Berg, J.-P. Lessard (Eds.), *Rigorous numerics in dynamics*, Vol. 74 of Proceedings of Symposia in Applied Mathematics, American Mathematical Society, Providence, RI, 2018, aMS Short Course: Rigorous Numerics in Dynamics, January 4–5, 2016, Seattle, Washington. doi:10.1090/psapm/074.
 URL <https://doi.org/10.1090/psapm/074>
- [74] J. B. van den Berg, J. Lessard, Rigorous numerics in dynamics, Notices Amer. Math. Soc. 62 (9) (2015) 1057–1061.
- [75] P. Zgliczynski, C^1 Lohner algorithm, Found. Comput. Math. 2 (4) (2002) 429–465. doi:10.1007/s102080010025.
 URL <https://doi.org/10.1007/s102080010025>
- [76] J. D. Mireles James, Validated numerics for equilibria of analytic vector fields: invariant manifolds and connecting orbits, (To appear in AMS lecture notes - winter short course series) (2017) 1–55.
- [77] S. Rump, INTLAB - INTerval LABoratory, in: T. Csendes (Ed.), *Developments in Reliable Computing*, Kluwer Academic Publishers, Dordrecht, 1999, pp. 77–104, <http://www.ti3.tu-harburg.de/rump/>.
- [78] X. Cabré, E. Fontich, R. de la Llave, The parameterization method for invariant manifolds. III. Overview and applications, J. Differential Equations 218 (2) (2005) 444–515.
- [79] A. Haro, M. Canadell, J.-L. s. Figueras, A. Luque, J.-M. Mondelo, *The parameterization method for invariant manifolds*, Vol. 195 of Applied Mathematical Sciences, Springer, [Cham], 2016, from rigorous results to effective computations. doi:10.1007/978-3-319-29662-3.
 URL <http://dx.doi.org.ezproxy.fau.edu/10.1007/978-3-319-29662-3>